Conte, Bruno

Working Paper

Climate Change and Migration: The Case of Africa

CESifo Working Paper, No. 9948

Provided in Cooperation with:
Ifo Institute – Leibniz Institute for Economic Research at the University of Munich

Suggested Citation: Conte, Bruno (2022) : Climate Change and Migration: The Case of Africa, CESifo Working Paper, No. 9948, Center for Economic Studies and ifo Institute (CESifo), Munich

This Version is available at:
https://hdl.handle.net/10419/265983

CESifo WORKING PAPERS

9948
2022

September 2022

Climate Change and Migration: The Case of Africa

Bruno Conte

CESifo

Impressum:

CESifo Working Papers
ISSN 2364-1428 (electronic version)
Publisher and distributor: Munich Society for the Promotion of Economic Research - CESifo GmbH
The international platform of Ludwigs-Maximilians University's Center for Economic Studies and the ifo Institute
Poschingerstr. 5, 81679 Munich, Germany
Telephone +49 (0)89 2180-2740, Telefax +49 (0)89 2180-17845, email office@cesifo.de
Editor: Clemens Fuest
https://www.cesifo.org/en/wp
An electronic version of the paper may be downloaded
· from the SSRN website: www.SSRN.com
· from the RePEc website: www.RePEc.org
· from the CESifo website: https://www.cesifo.org/en/wp

CESifo *Working Paper No. 9948*

Climate Change and Migration: The Case of Africa

Abstract

This paper estimates the impacts of climate change in sub-Saharan Africa (SSA) on migration and other economic outcomes. I develop a quantitative spatial model that captures the role of trade networks, migration barriers, and agricultural yields on the geography of the economy. I combine the model with forecasts of future crop yields to find that climate change, by the end of the century, reduces SSA real GDP per capita by 1.8 percent and displaces 4 million individuals. Migration barriers in SSA are very stringent: if absent, climate-induced migration exceeds 100 million individuals. Still, migration and trade are powerful adaptation mechanisms. Reducing migration barriers to the European Union (EU) standards eliminates the aggregate economic losses of climate change in SSA, but at the cost of more climate migration and higher regional inequality. Also reducing trade frictions to the EU levels attenuates this cost and makes SSA better off on aggregate and distributional terms.

JEL-Codes: O150, Q540, R120.

Keywords: climate change, migration, economic geography.

Bruno Conte
University of Bologna / Italy
b.conte@unibo.it
web: brunoconteleite.github.io

September 2022
I am indebted to my advisors Hannes Mueller and David Nagy for their constant support, guidance, and patience. I am also thankful to Gabriel Ahlfeldt, Donald Davis, Klaus Desmet, Remi Jedwab, Gabriel Kreindler, David Lagakos, Ishan Nath, Heitor Pellegrina, Giacomo Ponzetto, Esteban Rossi-Hansberg, Alessandro Ruggieri, Sebastian Sotelo, Jaume Ventura, and Yanos Zylberberg for useful comments and rich discussions along different stages of this project. Audiences at numerous seminars and confereces provided valuable feedback, to which I am also grateful. The usual disclaimers apply.

1 Introduction

One of the most concerning potential consequences of climate change is population displacement, recently coined as the *Great Climate Migration* (Lustgarten, 2020). Subsistence rural economies, like the sub-Saharan African (SSA henceforth) countries, lie at the center of this issue. They are agriculture-dependent economies whose populations are expected to increase remarkably during the next decades (United Nations and Social Affairs, 2019). Understanding how these economies would adjust to a climate-changing world, with potentially different crop yields, is crucial for identifying how this growing population will reallocate geographically.

Assessing the potential decisions of SSA economic agents when adapting to climate change is challenging. Changing agricultural yields could lead farmers to switch production towards alternative crops, yet remaining in the agricultural sector. Alternatively, they could sort out of agriculture, potentially moving geographically. Trade frictions would determine the extent to which specialization between agriculture and non-agriculture is feasible. Migration barriers would discipline the capacity of factors to reallocate geographically, potentially limiting sectoral reallocation. Thus, understanding how these forces (production switching, trade, and migration) respond to climate change is key to evaluating its impact on the economy.

In this paper, I develop a quantitative spatial model that accounts for these forces and can be used to quantify how their response to climate change translates into population displacement and economic losses. I take the model to a high-resolution ($1^\circ \times 1^\circ$ degree) geographical dataset that covers 42 countries of SSA. By simulating it for a future scenario by the end of the century, I estimate the aggregate and distributional impacts of climate change in terms of migration flows, welfare losses, and sectoral and spatial reallocation of production. In addition, I show that trade and migration are important adaptation mechanisms, and investigate the mitigating capacity of real-world trade and migration policies.

I begin by showing empirically that the expected changes in SSA agricultural yields for the future are heterogeneous across locations and crops. This will affect comparative advantages in agriculture differently for each crop, permitting local agricultural production to reshuffle across crops as a response to climate change.

Informed by this evidence, I develop a multi-sector quantitative spatial model that accommodates this mechanism. In the model, trade and migration between locations are costly. In each location, farmers produce goods from multiple agricultural sectors (crops) and firms produce non-agricultural goods. Differences in sectoral total factor productivities and market access across locations generate trade, shaping the spatial pattern of sectoral specialization. Relative sectoral prices and real income de-

termine sectoral expenditure shares, generating endogenous structural transformation through substitution and income effects.[1]

The model takes the perspective of subnational locations, so that trade and migration happen both within and across countries in SSA.[2] The intensity of the spatial frictions depends primarily on the distance between locations over the transportation network. However, they are also determined by country-level institutional factors. In particular, frictions for international trade are subject to an additional tariff-like cost. International migration is subject to an additional mobility cost related to barriers to foreign migrants at the destination country. Therefore, I map the model into real-world trade and migration policies, which allows me to investigate their role on the resulting climate change effects and the efficiency of alternative policy schemes.

To quantify the model, I assemble a $1^\circ \times 1^\circ$ degree spatial dataset on, among others, population, economic activity, transportation infrastructure, and agricultural production and suitability in SSA. Following Costinot et al. (2016), I model climate change as a shock to the suitability for growing crops. In practice, I draw on the GAEZ (IIASA and FAO, 2012) estimates of crop-specific potential yields for several grain crops in recent, past, and future (under climate change) periods. These potential yields reflect only local natural characteristics (e.g. topographic and climatic) and thus provide a measure of geographical natural advantages for growing a specific crop.[3,4] I also match the data to bilateral trade and migration flows at the country level.

I link the data to my model in three steps. First, I use the GAEZ yields for 2000 as the measure of the fundamental productivity for each crop. Second, I use transportation and geographical data to build an optimal trade network between all location pairs in SSA. Third, I quantify the unobserved fundamentals and parameters: the sets of fundamental productivities of the non-agricultural sector, sectoral productivity and preference shifters, amenities, country-level barriers to foreign migrants, and the degree of tariffs on international trade.[5] The latter two are quantified using country-level bilateral migration and trade data, thus capturing the strictness of the migration and trade policies in place in SSA as of 2000.

[1] I model preferences over agricultural and non-agricultural goods as nonhomothetic and assume the former to be a necessity (subsistence) good. Thus, my model features key aspects of structural change; in particular a downward slopping demand for agricultural goods with respect to income.

[2] Hence, I do not consider migration and trade with the rest of the world. The underlying motivation is that about 75% of international migrants from SSA countries (between 1990 and 2000) moved within SSA (Abel and Cohen, 2019). My model is however flexible and can be extended along this dimension.

[3] Hereafter, I refer to these potential yields as fundamental productivities/advantages indistinctly.

[4] To focus on subsistence agriculture, I consider only the main staple crops produced and consumed in the region (cassava, maize, millet, rice, sorghum, and wheat; see Table D.2). They account for 80% of the agricultural production, as of 2000, and 50% of the caloric intake in SSA (Porteous, 2019). An additional motivation for not considering cash crops is that I do focus on trade outside SSA.

[5] This last step requires the inversion of the spatial equilibrium so that the model achieves an exact fit of the data in terms of several characteristics of the SSA economy in 2000.

Next, I validate the calibrated model using a backcasting exercise. It consists of using the crop suitabilities for 1975 in a simulation whose outcome is contrasted with observable data. The model predicts well the grid cell-level changes in population between 2000 and 1975, reassuring its capacity of providing similar numbers for future periods. An additional overidentification test shows that the model identifies closely the degree of specialization in agriculture across countries.

My main counterfactual exercise consists of simulating a climate-changed SSA by the end of the century. I draw the estimates for crop yields in 2080 with climate change and simulate the model with them, keeping all other fundamentals unchanged.[6,7] The results show that climate change reduces SSA's real GDP per capita (the measure of welfare) by 1.8 percent and displaces 4 million individuals.[8] Most of the climate migrants move out of the Western Sahel and DR Congo, regions severely hit by climate change, into nearby countries like Nigeria or Tanzania. Damaged countries also experience large internal migration flows, and overall the population in country capitals increases. Importantly, the welfare results are very heterogeneous across space: the bottom and top deciles of the real GDP per capita change across countries are -6.5 and 6 percent, respectively, and some countries experience losses of up to 15 percent.

Moreover, climate change increases aggregate agricultural employment in SSA by about 0.85 percentage points. This happens because I model crops to be necessary (subsistence) goods. Thus, the economy responds to the reduced crop yields by allocating more labor into that sector (in order to produce the needed amount of agricultural goods). Nonetheless, this effect is spatially heterogeneous, and the direction of sectoral specialization roughly follows the relative changes in sectoral productivity (i.e. affected countries specialize out of agriculture, and the opposite for the least damaged). Interestingly, however, the resulting welfare effects across countries go in several directions and depend on a rich interaction between the forces driving migration, sectoral specialization, and trade.

I emphasize the role of these forces with additional simulations centered on the main mechanisms of the model. I start with bilateral migration frictions: eliminating them in the counterfactuals increases climate migration flows by more than 100 million individuals and reverses welfare losses (SSA real GDP per capita increases by 9.23 percent). That happens because lower mobility barriers boost the push-aspect of

[6]The GAEZ estimates are available for different hypothetical scenarios for the future. I pick the one that compares the closest to the most severe and pessimistic scenario: the Representative Concentration Pathway (RCP) 8.5. I check the robustness of my results to different scenarios in Section 6.4.

[7]The simulations for 2080 also account for the estimated future population growth. In the baseline, the fertility rates are taken exogenously from data by demographers. I however check the robustness of my results if allowing fertility to depend on climate change in Section 6.4.

[8]Population displacement is defined as the difference between the model-implied population, at the grid-cell level, of two simulations for 2080: with and without climate change. Grid-cells with positive values experience population inflows (or outflows if the opposite). See Section 6.1 for details.

climate change, reallocating labor out of unproductive rural regions and permitting a welfare-improving process of structural transformation. Importantly, these aggregate gains hide an underlying cost: the distribution of welfare changes across countries widens remarkably, with some countries experiencing losses larger than 30 percent. Thus, reducing mobility frictions poses a trade-off of reverting aggregate losses at the expense of higher regional inequality.

Next, I analogously investigate the role of two additional mechanisms in the model: trade and crop-switching. For the former, I find that trade openness reduces migration and welfare losses by providing more room for sectoral specialization. For the latter, I show that the capacity of producers to reallocate production across crops is a crucial margin of adaptation for SSA farmers. Ignoring this margin overestimates the productivity and welfare losses of climate change by not considering that crop yields are differently affected within locations.

I close my investigation with a policy experiment that assesses the potential mitigating role of migration and trade policies. I simulate a counterfactual scenario where migration and trade frictions in SSA drop to the levels of the European Union (EU). Doing so requires quantifying EU tariffs and country barriers to foreigners within the structure of the model (and using the result in the SSA simulations).[9] Adopting the migration policy of the EU eliminates the aggregate welfare losses in SSA at the cost of higher regional inequality. However, setting tariffs to EU levels on top of the migration policy attenuates that. In particular, the policy mix increases the efficiency of the allocation of factors across sectors and locations, which makes SSA better off both in aggregate and distributional terms. This last result has important policy implications: by combining both tools, SSA policymakers would take advantage of the changes in the climate and allow the economy to structurally change, through trade and migration, in a welfare-improving manner.

This paper contributes to three strands of the literature. One contribution is to a growing body of research that applies the tools of the quantitative spatial literature (e.g. Allen and Arkolakis, 2014; Redding, 2016; Redding and Rossi-Hansberg, 2017) to study the spatial aspects of the consequences of climate change, such as global warming (Desmet and Rossi-Hansberg, 2015; Conte et al., 2021; Cruz and Rossi-Hansberg, 2021; Rudik et al., 2021) and coastal flooding (Desmet et al., 2021; Balboni, 2021). My contribution is to incorporate, into a unique framework, a threefold set of features that are crucial to model climate migration in rural developing economies. First, by introducing labor mobility within and across countries into the framework of Costinot et al. (2016), I account for the heterogeneity of the climate shock across crops and show that

[9]More specifically, I build a likewise rich spatial dataset for the EU in 2000. I then link it to my model (with the same quantification procedure), retrieve the EU policy-related parameters (tariffs and country barriers to foreigners), and use them in the SSA simulations. See section 6.3 for details.

this dimension matters for understanding the migration and welfare consequences of climate change in SSA. Second, I allow for the subsistence aspect of agriculture to limit structural change as adaptation, as in Nath (2022) and Cruz (2021), but show that migration is a margin that attenuates this issue. Third, I account for real-world policies (tariffs and country-level barriers to foreign migrants) and show how they interact with sectoral specialization, trade, and the aggregate and distributional welfare effects of climate change.[10]

I also contribute to the macroeconomic literature centered on structural change (Duarte and Restuccia, 2010; Herrendorf et al., 2014; Comin et al., 2021) and its spatial aspects (Desmet and Rossi-Hansberg, 2014; Eckert and Peters, 2018; Fan et al., 2021; Fajgelbaum and Redding, 2022; Takeda, 2022). My core contribution is showing the role of climate change in incentivizing this process and the resulting aggregate and compositional welfare effects in SSA. Moreover, by showing the role of migration in that process, I also add to studies on the importance of reducing migration barriers in developing economies and their importance for structural change and development (Bryan and Morten, 2019; Caliendo et al., 2021; Morten and Oliveira, 2018; Lagakos et al., 2018). Along the same lines, my results on the mitigating role of trade policy add to a large literature on the importance of market integration for development (Asturias et al., 2019; Donaldson, 2018; Nagy, 2022; Ducruet et al., 2020; Sotelo, 2020; Atkin and Donaldson, 2015; Donaldson and Hornbeck, 2016; Atkin et al., 2021).

Lastly, I contribute to the current academic and policy research on future climate migration.[11] Several policy institutions produced results to guide policymakers in this matter, such as the Pulitzer Center (Lustgarten, 2020) and the World Bank (Rigaud et al., 2018). They use a partial equilibrium spatial framework that disregards several mechanisms present in my model, most notably bilateral migration barriers. Other related studies include Benveniste et al. (2020) and Burzyński et al. (2022), who model climate migration as a response to global warming and coastal flooding. My contribution lies in modeling the spatial links behind the adaptation decisions to climate change (where migration is a key mechanism of the long-run structural adjustment of the economy) and in providing policy-relevant results that are informative about the

[10]Naturally, there are aspects in this literature that my paper does feature. These include, among others, the absence of dynamics and the endogenous feedback between the economy and the climate. The reason for the former is data-driven: the GAEZ estimates are available for specific points in time (2000, 2050, and 2080) which inhibits modeling the transition towards the end of the century. The reason for the latter is that Africa emits about 3 percent of global CO_2 emissions, as of 2015, which makes it reasonable to assume that climate change is exogenous to economic activity.

[11]A large body of reduced-form research assesses the causal relationship between past weather shocks and migration in rural economies (Baez et al., 2017; Gröger and Zylberberg, 2016; Cai et al., 2016; Albert et al., 2021) and the resulting increasing urbanization (Barrios et al., 2006; Castells-Quintana et al., 2021; Henderson et al., 2017). Their results however cannot be extrapolated to the future and thus are not informative about potential future climate migration.

reach and interplay of migration and trade policies.

The rest of the paper is organized as follows. Section 2 describes the main data sources, and Section 3 documents a number of empirical facts related to the potential impact of climate change on SSA economy. Section 4 presents the theoretical framework. Section 5 details how the model is brought to the data, and Section 6 the results of the climate change counterfactuals, policy experiments, and several robustness checks. Section 7 concludes.

2 Data

I collect and aggregate several sources of geographical data within $1^\circ \times 1^\circ$ grid cells (about 100 km^2 at the equator), the empirical unit of observation. The set of cells covering 42 countries of SSA contains 2,007 cells. The sources, collection, and aggregation of the data follow below; see Appendix C for details.

GDP. Grid cell-level data on GDP per capita in US$ PPP (2000) comes from the Global Gridded Geographically Based Economic Data v4 (G-Econ, Nordhaus et al., 2006).

Population. The G-Econ database also provides the population count at the grid cell-level for 1990 and 2000. This was complemented with the gridded 1975 population data from the Global Human Settlement Project (GHSP, Florczyk et al., 2019). Finally, projections for future population at the country level for 2001–2100 were taken from United Nations and Social Affairs (2019).

Agricultural suitability. I construct a spatial and time-varying dataset of crop-specific suitabilities using the Food and Agriculture Organization's Global Agro-Ecological Zones database (GAEZ, IIASA and FAO, 2012). This data is generated by a state-of-the-art agronomic model that combines geographic characteristics (e.g. soil, elevation, etc.) with yearly climatic conditions to produce estimates of agro-climatic potential yields (at the 0.083 degrees resolution) for different crops and periods.[12] I collect and aggregate the potential yields for the 6 crops of interest for 1975, 2000, and 2080, with the latter based on estimates for a climate-changed world. The final data is a crop-cell level panel of potential yields for 1975, 2000, and 2080.

Agricultural production. Grid cell-level crop production comes from two sources: grid cell-level production data (in tonnes) for 2000 from GAEZ and country-level crop production (in current US$) for 2000-2010 from FAO-STAT. I convert current US$ to US$ PPP using their ratio on the G-Econ data.

[12]These potential yields, measured in tonnes/hectares, refer to the yield that a certain cell would obtain, on average, if its surface was fully devoted to a specific crop.

Transportation network. I build up a network connecting all grid cells of SSA by first combining the African extract of the Global Roads Open Access Data Set (gROADS, CIESIN, 2013)[13] with the transportation friction surface from the Accessibility to Cities project (Weiss et al., 2018).[14] As discussed in Section 5.2, this overcomes potential missing roads in some particular countries, and captures links between locations not necessarily through roads.

Bilateral trade and migration flows. Since bilateral trade and migration data at the grid-cell level does not exist, I focus on country flows. In particular, I extract the bilateral crop trade flows (in current US$, scaled to PPP as above) between all SSA country pairs from the International Trade and Production Database (ITPD-E, Borchert et al., 2021).[15] Moreover, I obtain the bilateral gross migration flows between SSA countries (between 1990 to 2000) from Abel and Cohen (2019)'s database.

3 Motivating facts

This section documents two facts about the potential impact of climate change in SSA. I establish that (i) these effects are expected to be strong and heterogeneous and, as such, (ii) potentially determinant in the future organization of the SSA economy. Overall, these facts provide empirical support for the channels I embed in the model.

Fact 1: Climate change is expected to bring about substantial and spatially heterogeneous changes in agricultural suitability in SSA.

I use the GAEZ estimates of agro-climatic potential yields for 2000 and 2080 to show the expected degree of severity and heterogeneity in climate change's impact.[16] I define ΔA_i^k as the changes in the yields of crop k (in tonnes/ha) in location i between the two periods, and ΔA_i as the average change within locations.

Panel A of Figure 1 illustrates the high level of heterogeneity in the average climate change shock to agricultural yields. In terms of levels, several locations will become less suitable for agriculture, with average yields declining by 3 tonnes/ha (50 percent

[13]This data aggregates the best available public-domain road data by country into a global roads coverage database. Because the data is gathered from different sources, the period of the road network representations ranges from the 1980s to 2010, depending on country.

[14]This high-resolution surface (0.01 degrees resolution) provides the instantaneous cost of passing through a cell conditional on geographical features (e.g. type of terrain, steepness, etc.) as well as infrastructure (whether the cell is on a road, railroad, river, etc.).

[15]The ITPD-E closely tracks the traded sectors globally and is thus a data benchmark for statistical estimation. In particular, the ITPD-E contains consistent data on international and domestic trade for 243 countries and 170 industries between 2000 and 2016.

[16]The 2080 GAEZ forecasts are calculated assuming a hypothetical scenario for the future evolution of the world's climate. Appendix C.1 describes how I chose the scenario from which to draw the data in order that the results come closest to Representative Concentration Pathway (RCP) 8.5.

Figure 1: Expected impact of climate change on average crop yields (left) and the standard deviation of crop-yield changes (right) in SSA between 2000 and 2080

Panel A: Change in average suitability to agriculture.

Panel B: Standard deviation of changes in crop suitabilities at the location level.

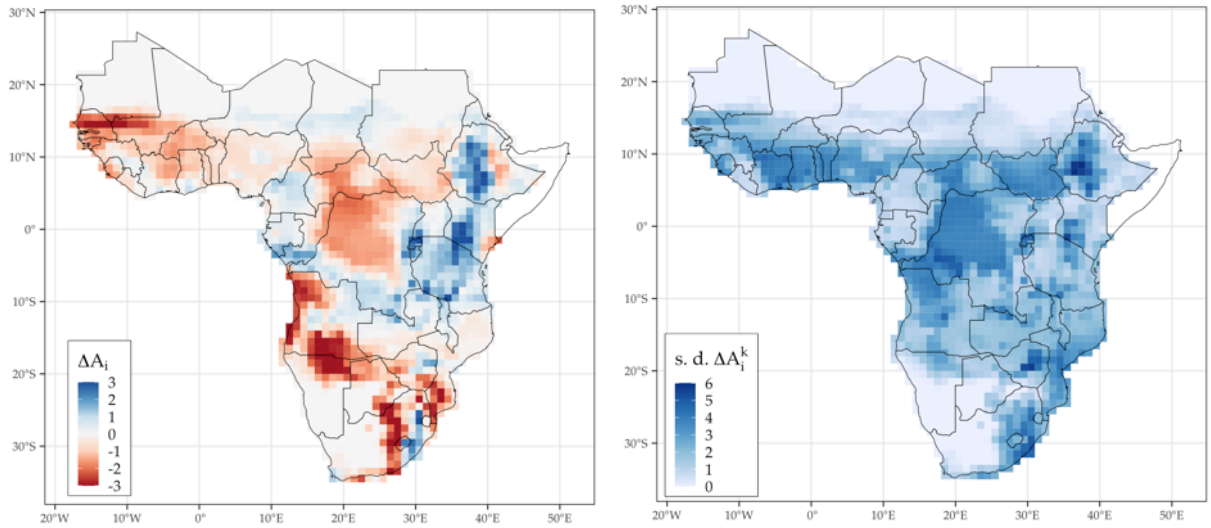

Notes: Panel A shows the estimated change (truncated for ease of visualization) in average potential yields between 2000 and 2080. Panel B shows the standard deviation of the crop-level yield changes within cells. See Section 2 and Appendix C for details.

of average yields) or more. However, other locations will become more suitable and to a similar extent. This finding contradicts a general view of climate change as a spatially homogeneous shock.

To illustrate the heterogeneity across crops, Panel B of Figure 1 documents the dispersion of climate change effects at the cell level (in standard deviations of ΔA_i^k). The changes in yields are not homogenous across crops, differentially shifting the relative ranking of crop suitabilities within cells. Hence, climate change will affect agricultural comparative advantages heterogeneously across both space and crops.

Thus, adjusting crop choices is a potential coping margin for affected farmers in SSA. However, the extent to which such Ricardian production adjustments can take place in SSA depends on the strength of these natural comparative advantages in shaping effective agricultural production. The next empirical fact provides evidence that such a mechanism indeed exists and emphasizes the importance of embedding it in my theoretical framework.

Fact 2: Natural crop suitability explains to a large degree the patterns of crop specialization within and across countries in SSA.

Figure 2 shows how observed production in 2000 correlates with the GAEZ yields. In particular, Panel A plots crop production against the yields at the location-crop level. The raw data values are first net out of location and country-crop fixed effects, so

Figure 2: Comparative advantage and the organization of the SSA economy: relationship of crop yields with effective production

Panel A: Grid cell-level crop production. *Panel B:* Country-level crop production.

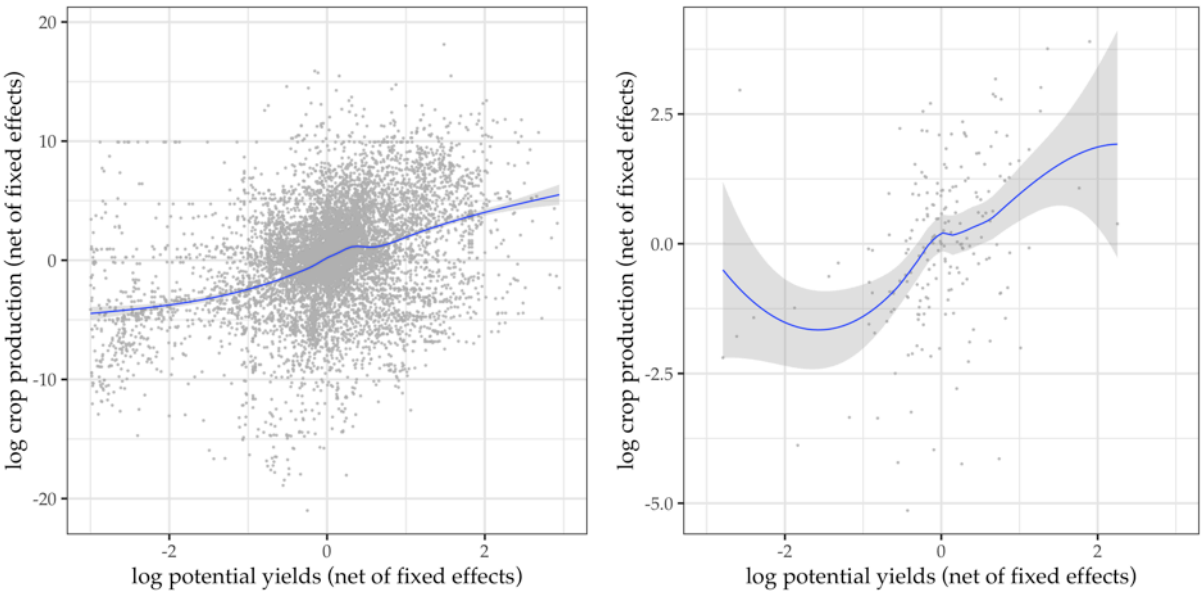

Notes: Panel A (B) plots the correlation between GAEZ potential yields and effective grid cell-level (country-level) production. The blue line stands for an estimated polynomial regression, and grey-shaded areas the 95% confidence bands.

that confounding factors at both levels are controlled for. There is a strong correlation between natural advantages and effective production. As robustness, Panel B shows a likewise positive correlation between country-level crop production and average crop suitability within countries.[17]

Overall, the data conveys a sound message: crop specialization happens both across and within countries. To generate this pattern, my general equilibrium model will take the perspective of subnational units that specialize in (and trade) crops based on comparative advantage.

4 Model

This section describes a static quantitative spatial model that quantifies the general equilibrium impacts of future climate change. It provides a tractable framework to account for the role of geographical heterogeneity along several dimensions (i.e. sectoral productivities, market access, and migration barriers, among others) in determining the spatial distribution of economic activity and population.[18]

[17]The grid cell-level production data is also produced by the GAEZ agro-climatic model. Thus, production and crop yield data could be (hypothetically) mechanically correlated. The FAOSTAT country-level data, obtained from national statistics, would not incorporate such a hypothetical correlation.

[18]Refer to Appendix A for further details and derivations of the model.

4.1 Environment

The economy S is composed by N locations, denoted by i, j, or s. Each i belongs to a country $c(i) \in \{1, ..., C\}$ and is initially populated by $L_i^0 \in \{L_i^0\}_{i \in S} \equiv \mathcal{L}$ of workers who supply their labor inelastically. There are K sectors $k \in \{1, ..., K\}$ in the economy: $K-1$ crops and a non-agricultural composite K sector. Locations can produce a locally differentiated variety of each sector's goods. Each location has a sector-specific fundamental productivity parameter $A_i^k \in \mathcal{A} = \{A_1^1, ..., A_N^K\}$ that partially drives the degree of comparative advantage across space in each sector. Moreover, workers residing in i enjoy an amenity value $u_i \in \{u_i\}_{i \in S} \equiv \mathcal{U}$.

Goods and labor units are mobile in S, subject to frictions. In particular, $\mathcal{T} = \{\tau_{ij}\}_{i,j \in S}$ is the bilateral trade friction matrix where $\tau_{ij} = \tau_{ji} \geq 1$ represents the units required to ship 1 unit of good from location i to j. Frictions in labor mobility depend on an analogous bilateral migration cost $\bar{m}_{ij} \in \mathcal{M}$ and on an idiosyncratic taste shock to the migration choices of agents.

The geography of the economy is the set $\mathcal{G}(S) = \{\mathcal{L}, \mathcal{A}, \mathcal{U}, \mathcal{T}, \mathcal{M}\}$, i.e. the spatial fundamentals that interact with the economic forces of the model and determine the spatial distribution of the economic activity. In what follows, I describe how the economic component is structured.

Technology and Market Structure. In every location i, a representative firm produces goods of each sector k with labor as the unique input of the following linear production function:

$$q_i^k = b_i^k A_i^k L_i^k, \tag{1}$$

where b_i^k stands for a location-sector efficiency shifter unrelated to i's natural advantage in producing sector k goods (e.g. technology adopted in production). The output can be locally consumed or traded with other locations. Trade takes place in a perfectly competitive framework with full information. Thus, the price of the sector k variety produced in i and shipped to location j is given by:

$$p_{ij}^k = (w_i / b_i^k A_i^k) \times \tau_{ij}, \tag{2}$$

where the first and second subscripts stand for, respectively, the production and consumption locations, and w_i is the wage in location i.

Preferences. Each location i is initially populated by a continuum of heterogeneous workers who decide where to live and how much to consume of the varieties of the K sectors. In particular, a worker v initially living in location i who decides to migrate to j enjoys

$$U_{ij}(v) = C_j \times \bar{m}_{ij}^{-1} \times \varepsilon_j(v), \tag{3}$$

where C_j stands for the utility obtained from consumption in j and $\bar{m}_{ij}$ is the mobility cost of migrating to j. Moreover, v's final utility is affected by a destination taste shock $\varepsilon_j(v)$, which disciplines workers' heterogeneous taste with respect to their preferred destination.

Consumption choice. Workers in a location j decide how much to consume of all possible i varieties of goods from all K sectors, $\{q_{ij}^k\}_{i,k}$. Their preferences feature love for varieties, which is modeled using a sectoral CES tier:

$$C_j^k = \left(\sum_{i \in \mathcal{S}} \left(q_{ij}^k \right)^{\frac{\eta_k - 1}{\eta_k}} \right)^{\frac{\eta_k}{\eta_k - 1}}. \tag{4}$$

Each worker earns wage w_j, so that $\sum_{i \in S} \sum_{k \in \mathcal{K}} p_{ij}^k q_{ij}^k = w_j$ is the budget constraint of a worker living in j. Utility maximization with respect to consumption implies that the share of j's spending on i's variety of sector k is

$$\lambda_{ij}^k = \frac{p_{ij}^k q_{ij}^k}{\sum_{i \in S} p_{ij}^k q_{ij}^k} = \left(p_{ij}^k / P_j^k \right)^{1 - \eta_k}, \text{ where} \tag{5}$$

$$P_j^k = \left(\sum_{i \in \mathcal{S}} \left(p_{ij}^k \right)^{1 - \eta_k} \right)^{\frac{1}{1 - \eta_k}} \tag{6}$$

is the Dixit-Stiglitz price index of sector k at j and $\eta_k > 1$ sector k's Armington CES. Thus, workers devote a larger expenditure share to varieties from the cheapest suppliers (with the lowest p_{ij}^k). The sectoral CES η_k determines the extent to which this occurs: the larger it is, the more substitutable varieties within crop k become, and the larger the share of expenditure on the cheapest supplier.

Worker choices across the $K - 1$ crops have a similar form. All crop CES composites are further aggregated into an agricultural CES tier (denoted by a):

$$C_j^a = \left(\sum_{k \neq K} \left(C_j^k \right)^{\frac{\gamma_a - 1}{\gamma_a}} \right)^{\frac{\gamma_a}{\gamma_a - 1}}. \tag{7}$$

$\gamma_a > 1$ is the CES between crops which drives their degree of substitutability. Following (5), j's share of expenditure on crop k relative to total crop expenditure is:

$$\Xi_j^k = \left(P_j^k / P_j^a \right)^{1 - \gamma_a}, \text{ where} \tag{8}$$

$$P_j^a = \left(\sum_{k \neq K} \left(P_j^k \right)^{1 - \gamma_a} \right)^{\frac{1}{1 - \gamma_a}} \tag{9}$$

is the price index of the aggregate agricultural sector a. Therefore, workers also substitute crops based on their relative prices. Larger values of γ_a imply more consumption of the locally cheapest crop and a stronger degree of specialization in crop consumption across locations.

Finally, the consumption choice between agricultural and non-agricultural goods is modeled with a further nonhomothetic CES tier in the spirit of Comin et al. (2021). In particular, the utility from consuming goods, C_j, is implicitly determined from:

$$\sum_{k\in\{a,K\}} \left(\Omega^k\right)^{1/\sigma} \left(C_j\right)^{\epsilon_k/\sigma} \left(C_j^k\right)^{(\sigma-1)/\sigma} = 1, \tag{10}$$

where $\sigma > 0$ is the CES between the a and K aggregate sectors, ϵ_k is their nonhomothetic elasticity of substitution, and Ω_k are sectoral preference shifters. Utility maximization implies that total consumption equals real wages, i.e. $C_j = w_j/P_j$ in each location j. Moreover, price indexes and expenditure shares are respectively determined as:

$$P_j = \left(\sum_{k\in\{a,K\}} \left(\Omega^k \left(P_j^k\right)^{1-\sigma}\right)^{\frac{1-\sigma}{\epsilon_k}} \times \left(\mu_j^k w_j^{1-\sigma}\right)^{\frac{\epsilon_k-(1-\sigma)}{\epsilon_k}}\right)^{\frac{1}{1-\sigma}}, \text{ and} \tag{11}$$

$$\begin{aligned}\mu_j^k &= P_j^k C_j^k / w_j \\ &= \Omega^k \times \underbrace{\left(P_j^k/P_j\right)^{1-\sigma}}_{\text{substitution}} \times \underbrace{\left(w_j/P_j\right)^{\epsilon_k-(1-\sigma)}}_{\text{nonhomotheticity}} \quad \forall k \in \{a, K\}.\end{aligned} \tag{12}$$

Equation (12) shows that workers' choices between agricultural and non-agricultural goods are more complex than within agriculture. The reasons are two: first, it contains a substitution component analogous to eqs. (5) and (8) that nevertheless permits a lower degree of substitutability between sectors ($\sigma < 1$). That makes it possible for changes in sectoral expenditures to be relatively lower (in magnitude) than the changes in relative prices. Second, it features a nonhomothetic component that maps changes in real income onto changes in sectoral expenditure shares – essentially, an income effect. The elasticities ϵ_k determine this relation: if $\epsilon_k < 1-\sigma$, then sector k goods are a necessity whose expenditure decreases with income(and the opposite if $\epsilon_k > 1-\sigma$). Note that if $\epsilon_k = 1-\sigma$ for all k, then the nonhomothetic component vanishes and eqs. (11) and (12) become isomorphic to eqs. (8) and (9).[19]

In equilibrium, the per capita demand for i variety of sector k goods in j is

[19]Such a demand structure is required in order to account for the necessity (subsistence) aspect of agricultural goods when endogenizing sectoral shifts from agriculture to non-agriculture (i.e. structural change). This is what Gollin et al. (2007) refer to as the food problem and what Nath (2022) shows to be a limitation of structural change as a response to climate change. I discuss this further in Section 4.3.

$q_{ij}^k = \lambda_{ij}^k \Xi_j^k \mu_j^a w_j$ for crops and $q_{ij}^K = \lambda_{ij}^K \mu_j^K w_j$ for the K^{th} sector. Therefore, the total expenditure in j on goods produced in i, X_{ij}, is defined as:

$$\begin{aligned} X_{ij} &= \sum_{k \in \mathcal{K}} X_{ij}^k = \sum_{k \neq K} \lambda_{ij}^k \Xi_j^k \mu_i^a w_j L_j + \lambda_{ij}^K \mu_j^K w_j L_j \\ &= \sum_{k \neq K} \left(\frac{w_i \tau_{ij}}{b_i^k A_i^k P_j^k} \right)^{1-\eta_k} \left(\frac{P_j^k}{P_j^a} \right)^{1-\gamma_a} \Omega^a \left(\frac{P_j^a}{P_j} \right)^{1-\sigma} \left(\frac{w_j}{P_j} \right)^{\epsilon_a - (1-\sigma)} w_j L_j + \\ &+ \left(\frac{w_i \tau_{ij}}{b_i^K A_i^K P_j^K} \right)^{1-\eta_K} \Omega^K \left(\frac{P_j^K}{P_j} \right)^{1-\sigma} \left(\frac{w_j}{P_j} \right)^{\epsilon_K - (1-\sigma)} w_j L_j. \end{aligned} \tag{13}$$

Location choice. Workers choose where to live in order to maximize utility. In particular, worker v initially living in i chooses a destination j in order to solve:

$$\max_j \quad U_{ij}(v) = \left(w_j / P_j \right) \times \bar{m}_{ij}^{-1} \times \varepsilon_j(v). \tag{14}$$

Therefore, workers will prefer locations with higher real wages, although subject to the bilateral migration cost $\bar{m}_{ij}$ and the destination taste shock $\varepsilon_j(v)$. Formally, the former is modeled as

$$\bar{m}_{ij} = m_{ij} \times m_{c(j)} \text{ if } c(i) \neq c(j), \text{ and } \bar{m}_{ij} = m_{ij} \text{ otherwise,} \tag{15}$$

where m_{ij} and $m_{c(j)} \geq 1$. Thus, mobility costs depend on m_{ij} (which accounts for bilateral characteristics like distance) and potentially $m_{c(j)}$. The latter matters only if the location choice requires workers to switch countries. Hence, it captures country-specific characteristics of destination j in terms of national barriers to foreigners.

Moreover, I assume that the taste shock is drawn independently (across workers and locations) from an extreme-value distribution with shape parameter $\theta > 0$ and scale parameter $u_i L_i^{-\alpha}$. That is,

$$\varepsilon_j \sim G_j(z) = e^{-z^{-\theta} \times \left(u_j L_j^{-\alpha} \right)}. \tag{16}$$

The parameter θ drives workers' heterogeneity with respect to their location tastes (and, to some extent, the dispersion forces in the economy). A higher θ makes agents more homogeneous and their location decisions more dependent on real wages w_j / P_j. That drives down the dispersion forces in the economy. In contrast, a lower θ implies greater heterogeneity among agents who are more likely to draw higher values of taste shocks for every location. In that case, dispersion forces increase. Moreover, the scale parameter $u_j L_j^{-\alpha}$ determines the average of the preference draws; u_j stands for the fundamental amenity of destination j; and $\alpha > 0$ determines the extent to which

population density diminishes quality of life.

The distributional assumption on taste preferences allows for a closed-form solution to the location choice of workers. Following Eaton and Kortum (2002), the share of workers initially in i who choose to move to j is equivalent to:

$$\Pi_{ij} = \mathbb{P}\left(W_j(v) \geq \max\{W_s(v)\}_{s \neq j} \right) = \frac{(w_j / P_j)^{\theta} \bar{m}_{ij}^{-\theta} u_j L_j^{-\alpha}}{\sum_{s \in S} (w_s / P_s)^{\theta} \bar{m}_{is}^{-\theta} u_s L_s^{-\alpha}}. \tag{17}$$

Therefore, the total number of workers that choose to live in destination j is:

$$L_j = \sum_{i \in S} \Pi_{ij} \times L_i^0. \tag{18}$$

This is an intuitive result: locations with higher real wages (w_j / P_j) and/or density-adjusted amenities $(u_j L_j^{-\alpha})$ will have a higher population in equilibrium. The magnitude of this effect is partially driven by θ, which is the elasticity of the location choice with respect to real wages and to bilateral migration costs.

4.2 Spatial equilibrium

Given the geography $\mathcal{G}(S)$ and the exogenous parameters $\Theta \equiv \{\Omega_k, \eta_k, \gamma_a, \epsilon_k, \sigma, \theta, \alpha\}$, a spatial equilibrium is a vector of factor prices and labor allocations $\{w_j, L_j\}_{j \in S}$ such that eqs. (2), (6), (9), (11) to (13) and (18) hold, and markets for goods clear. Formally, market clearing requires that each j's wage bill equals total exports to and total imports from all locations $i \in S$, including itself. That is,

$$w_j L_j = \sum_{i \in \mathcal{S}} X_{ji} = \sum_{i \in \mathcal{S}} X_{ij}. \tag{19}$$

This condition is equivalent trade-balancing in all locations. Note that factor markets clearing is determined by eq. (18), since $\Sigma_i \Pi_{ij} = 1$ for all j by construction. Moreover, by using eq. (13) on (19), one characterizes the spatial equilibrium with the following

system of $6 \times N$ equations and unknowns:

$$w_j L_j = \sum_{i \in S} \sum_{k \neq K} \left(\frac{w_i \tau_{ij}}{b_i^k A_i^k P_j^k} \right)^{1-\eta_k} \left(\frac{P_j^k}{P_j^a} \right)^{1-\gamma_a} \Omega^a \left(\frac{P_j^a}{P_j} \right)^{1-\sigma} \left(\frac{w_j}{P_j} \right)^{\epsilon_a - (1-\sigma)} w_j L_j + \\ + \sum_{i \in S} \left(\frac{w_i \tau_{ij}}{b_i^K A_i^K P_j^K} \right)^{1-\eta_K} \Omega^K \left(\frac{P_j^K}{P_j} \right)^{1-\sigma} \left(\frac{w_j}{P_j} \right)^{\epsilon_K - (1-\sigma)} w_j L_j \tag{20}$$

$$P_j = \left(\sum_{k \in \{a,K\}} \left(\Omega^k \left(P_j^k \right)^{1-\sigma} \right)^{\frac{1-\sigma}{\varepsilon_k}} \left(\mu_j^k w_j^{1-\sigma} \right)^{\frac{\varepsilon_k - (1-\sigma)}{\varepsilon_k}} \right)^{\frac{1}{1-\sigma}} \tag{21}$$

$$P_j^k = \left(\sum_{i \in S} (w_i \tau_{ij} / b_i^k A_i^k)^{1-\sigma} \right)^{\frac{1}{1-\sigma}} \tag{22}$$

$$P_j^a = \left(\sum_{k \neq K} \left(P_j^k \right)^{1-\gamma_a} \right)^{\frac{1}{1-\gamma_a}} \tag{24}$$

$$L_j = \sum_{i \in S} \frac{(w_j / P_j)^\theta \bar{m}_{ij}^{-\theta} u_j L_j^{-\alpha}}{\sum_{s \in S} (w_s / P_s)^\theta \bar{m}_{is}^{-\theta} u_s L_s^{-\alpha}} \times L_i^0 \tag{23}$$

$$\mu_j^k = \Omega^k \left(P_j^k / P_j \right)^{1-\sigma} \left(w_j / P_j \right)^{\epsilon_k - (1-\sigma)} \tag{25}$$

I solve this high-dimensional, non-linear system of equations with the iterative algorithm described in Appendix A.4, where I also discuss aspects related to the existence and uniqueness of the equilibrium and practical aspects of the counterfactuals using the calibrated model.

4.3 Illustration and discussion of the underlying mechanisms

I illustrate how changes in the fundamentals shape the geographical distribution of economic activity and population by representing it as a line with a discrete number of locations. By doing so, I emphasize the effect of the model's underlying mechanisms on the agent's mobility decisions in response to a climate shock to the economy.

The locations $i \in \{1, ..., N\}$ are distributed over a line and are homogeneous with respect to amenities, efficiency shifters, and initial population ($u_i = u$, $b_i^k = b$, and $L_i^0 = l \; \forall i, k$). The economy is composed of two countries, where the ten left-most locations stand for country 1. I initially set $K = 2$, so that the agricultural a sector consists of one crop only. I assume that the distribution of sectoral fundamental productivities is increasing in the right-most locations and that every location is more productive in the K^{th} sector. I also set bilateral trade and mobility frictions to be proportionate to the bilateral distances and make it costly to migrate to country 2. In terms of preferences, I assume that the agricultural crop is a necessity good and the opposite for the K^{th} sector.[20]

[20] That is, $\epsilon_a < 1 - \sigma$ and the opposite for $k = K = 2$. Other values for this economy are $m_1 = 1$,

Figure 3: Equilibrium values of $\{L_i^1, L_i^2\}_{i \in S}$ for an economy represented on a line

Panel A: Migration barriers, sectoral specialization, and CΔ.

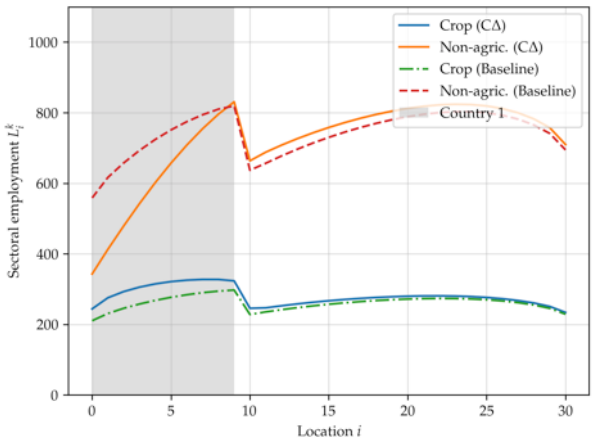

Panel B: CΔ, the food problem, and the role of trade frictions.

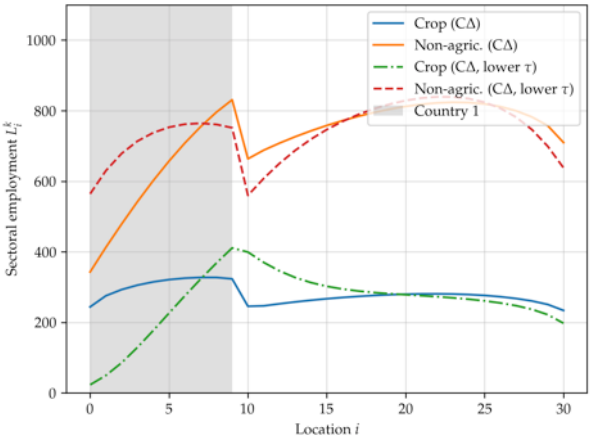

Panel C: CΔ and migration barriers.

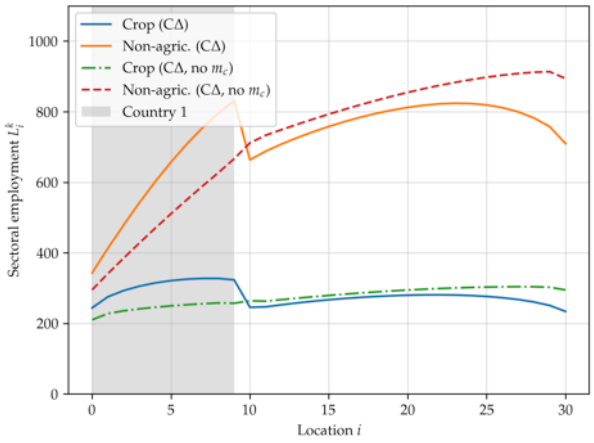

Panel D: CΔ and crop switching.

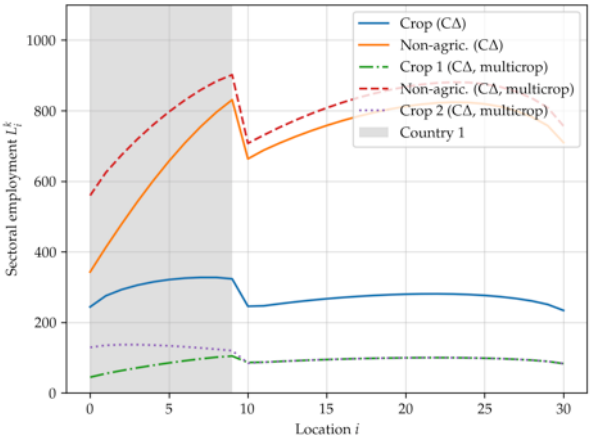

Notes: Equilibrium labor allocations for the model described in Section 4.3. Panel A describes the equilibrium of the baseline and climate change simulations (country 1 becomes less suitable for crops). Panel B, C, and D plot the results of the climate change scenario with, respectively, lower trade frictions (a reduction in τ), no migration barriers between countries ($m_c = 1$ for all c) and multiple crops ($K = 3$).

Panel A of Figure 3 plots the equilibrium distributions of $\{L_i^k\}$ as dashed lines (baseline). Overall, the economy produces more non-agricultural goods, which is the most productive sector. In distributional terms, the rightmost locations in each country have a higher level of economic activity and a larger population. The discontinuity at the country boundaries (i = 10) illustrates the role of country migration barriers (i.e. $m_2 > 1$). There is a higher population density on country 1's side due to the inability of workers to cross into country 2, where productivities and real wages are higher.

Subsequently, I simulate a climate shock by reducing country 1's crop productivities even further. The result is shown in Panel A of Figure 3 using solid lines (CΔ). Country 1 changes its patterns of sectoral specialization by increasing its relative em-

$m_2 = 1.5$, $\tau_{ij} = m_{ij} = e^{\tau \times |i-j|}$, and $A_i^k = a_k \times i$, where $\tau = 0.05$ and $a_2 > a_1$.

ployment in agriculture. This is driven by the necessity aspect of agricultural goods. Climate change reduces crop productivity in country 1, which reacts by increasing agricultural employment so to produce the needed quantity of crops. This reduces real income in that country, increasing its share of expenditure on crops. Country 2, if anything, gets benefitted. Its population and non-agricultural employment increase due to the climate migrants from country 1.

This simple exercise illustrates the limitations of structural transformation as a response to climate change. As rightly argued by Nath (2022), economies will switch production out of affected sectors only if capable of importing subsistence goods from unaffected regions. He refers to this as the food problem, inspired by previous studies of structural change and development (Gollin et al., 2007; Herrendorf et al., 2014). Panel B of Figure 3 provides further quantitative evidence of how this mechanism works in my model. When facing lower trade frictions, country 1 switches production out of agriculture, since it can now outsource crops from the nearest locations in country 2 (which shifts its production towards agriculture).

The novelty of my framework lies in the addition of two dimensions that further interact with the mentioned adaptation mechanisms. The first is migration barriers, whose role is illustrated in Panel C of Figure 3 (the climate change scenario without country migration barriers, i.e. $m_c = 1$ for all c). The results are intuitive: instead of reacting to the food problem, workers in country 1 migrate to country 2. Overall, workers enjoy higher real wages and spend lower income shares on agricultural goods, making climate change less of a problem. Thus, migration can have a welfare-improving role as a response to climate change. It permits individuals to move out of unproductive rural regions, allowing for a more efficient sectoral spatial sorting of workers. This echoes the insights obtained from research on spatial structural change (Eckert and Peters, 2018) and on the gains from lowering migration barriers in rural developing economies (Bryan and Morten, 2019; Lagakos et al., 2018; Pellegrina and Sotelo, 2021).

The second additional dimension is the multi-crop aspect of the agricultural sector. Crops are partial substitutes as subsistence, and Section 3 shows that climate change is expected to alter their yields heterogeneously within locations. Thus, a potential response of farmers in affected locations would be to switch production towards less-affected crops. The role of this margin is shown in Panel D of Figure 3. Dashed lines represent the outcomes of a simulation with two crops, where only crop 1 is affected in country 1. As a result, locations in that country switch production towards (unaffected) crop 2. This increases non-agricultural employment, real wages and welfare. Country 2 remains qualitatively unaffected, and overall the economy is better off relative to the one-crop scenario.

5 Bringing the model to the SSA data

I calibrate the model to match SSA data for the year 2000. To do so, I use a mix of calibration and parametrization methods that map the model to observable features of the SSA economy. The goal is to quantify the parameters Θ and the fundamentals $\mathcal{G}(S)$. Table 1 summarizes the methods and sources used. Section 5.6 documents the results of a number of overidentification tests that validate the calibrated model.[21]

5.1 Preference parameters

I draw the values for the preference parameters $\{\eta_k, \gamma_a, \epsilon_k, \sigma, \theta, \alpha\}$ from the related literature. I set the lower-tier CES as $\eta_k = 9.5$ for crops and $\eta_K = 5.5$ (as in Pellegrina and Sotelo, 2021; Caliendo and Parro, 2015), and the mid-tier CES as $\gamma_a = 2.5$ (following Sotelo, 2020). As for the upper-tier nonhomothetic CES, I follow Nath (2022) and set $\sigma = 0.27$, $\epsilon_a = 0.29$, and $\epsilon_K = 1$. Therefore, agricultural goods in my framework are a necessity, as opposed to non-agricultural K goods. Finally, I set $\theta = 2$ and $\alpha = 0.32$ following Monte et al. (2018) and Desmet et al. (2018), respectively.

5.2 Transportation network and trade costs

I follow the related literature (e.g. Allen, 2014; Donaldson, 2018; Pellegrina, 2022), by assuming that trade frictions are proportional to the travel distance between locations:

$$\tau_{ij} = \text{distance}(i,j)^{\delta} \times \tau_{ij}^{F}, \tag{26}$$

where $\text{distance}(i,j)$ stands for the shortest bilateral distance between the two locations and $\tau_{ij}^{F} \geq 1$ for an additional tariff-like trade friction. That is, $\tau_{ij}^{F} > 1$ only if $c(i) \neq c(j)$.

To calculate the distances between all location pairs, I first overlay the gROADS road network data onto the Accessibility to Cities friction surface data and set the lowest value for the pixels over the roads.[22] I then use a pathfinding algorithm to calculate the shortest routes and respective distances between all neighboring cells.[23] With these distances in hand, I use the Dijkstra algorithm to calculate the shortest distance between all location pairs. To map these distances onto $\mathcal{T}$, in line witheq. (26),

[21] In addition, Appendix A.5 discusses the data used and the numerical algorithms implemented, while Appendix A.6 discusses the implications of the parameter values drawn from the literature.

[22] The advantage of this strategy is that it provides additional information for my algorithm in the case of routes between coordinates not linked by roads. My method "connects" to a road by way of an optimal path with respect to topography, which is more realistic than assuming a linear path to the closest road.

[23] I obtain the coordinates of each cell from the longitude and latitude of the most populated settlement/city in each cell. See Appendix C for more details and fig. D.3 for the results.

Table 1: Fundamentals, parameters, estimation methods and sources from the literature

Parameters	Description	Reference / Moment matched
$\eta_k = 9.5$	Lower-tier CES ($k \neq K$, crops)	Pellegrina and Sotelo (2021)
$\eta_K = 5.5$	Lower-tier CES (non-agriculture)	Pellegrina and Sotelo (2021)
$\gamma_a = 2.5$	Mid-tier CES (across crops)	Sotelo (2020)
$\sigma = 0.26$	Upper-tier CES	Nath (2022)
$\varepsilon_a = 0.29$	Non-homoth. CES (agriculture)	Nath (2022)
$\varepsilon_K = 1$	Non-homoth. CES (non-agriculture)	Nath (2022)
$\{\Omega_k\}_{a,K}$	Sectoral preference shifters	Aggregate sectoral expenditure
$\theta = 2$	Workers' (inverse) heterogeneity	Monte et al. (2018)
$\alpha = 0.32$	Congestion to population density	Desmet et al. (2018)

Fundamentals	Subset	Description	Data source / Moment matched
$\mathcal{L}$	-	SSA's initial population	Population data in 2000 and 1990
$\{b_i^k\}_{i \in S}$	-	Productivity shifters	Matched to location-sector production data in US$
$\mathcal{A}$	$\{A_i^k\}_{i \in S, k \neq K}$	Agricultural productivities	GAEZ data
	$\{A_i^K\}_{i \in S}$	Non-agricultural productivities	Matched to GDP data in US$
$\mathcal{U}$	-	Amenities	Matched to population data
$\mathcal{T}$	dist(i,j)	Bilateral travel distance	Transportation data
	$\delta = 0.3$	Distance elasticity of τ	Moneke (2020)
	$\tau_{ij}^F = 2.175$	Tariff-like trade friction	Matched to aggregate trade flows in US$
$\mathcal{M}$	dist(i,j)	Bilateral travel distance	Transportation data
	$\phi = 0.5$	Distance elasticity of m_{ij}	Matched to total internal migration data
	$\{m_c\}_{c=1}^C$	Country migration barriers	Matched to country migration data (from bilateral flows)

Figure 4: Estimated trade network for SSA – Western and Eastern Africa

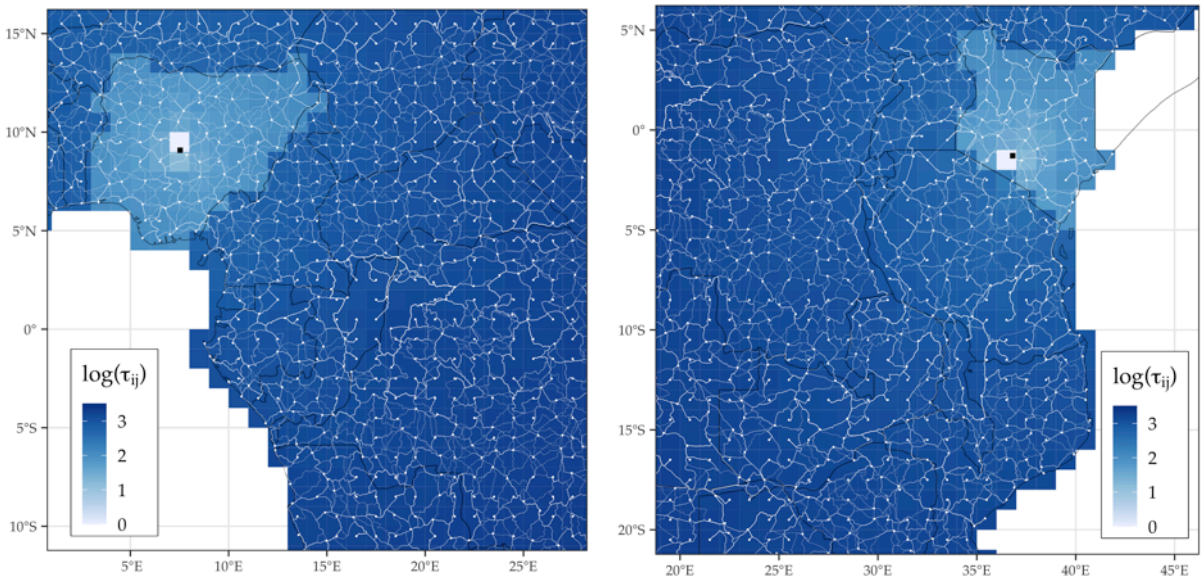

Notes: Notes: Estimated trade network for Western Africa (left) and Eastern Africa (right). The network is built by finding the shortest path between all neighboring cells over the road infrastructure. τ_{ij} represents the estimated iceberg trade costs with respect to the capital of Nigeria (left) and the capital of Kenya (right), both represented by a black dot. See Section 5.2 for details.

I first I set $\delta = 0.3$ following Moneke (2020). I then calibrate $\tau_{ij}^F = 2.175$ by matching the model-generated aggregate trade flows to the observed data. This last step is done simultaneously with the calibration of other fundamentals, as explained in Section 5.3.

Figure 4 illustrates a subsample of the calibrated $\mathcal{T}$. It shows the complexity of the trade network, which replicates well the existing transportation infrastructure both within and across countries. As expected, trade frictions increase with distance. Moreover, the discontinuity of the gradient is evidence of the additional cost of international trade captured by the parameter τ_{ij}^F.

5.3 Fundamental productivities, sectoral shifters, and tariffs

The set of fundamentals and parameters $\{\mathcal{A}, b_i^k, \Omega_k, \tau_{ij}^F\}_{i,j,k}$ are quantified as follows. First, I use the agro-climatic yields from GAEZ as the fundamental productivities of the agricultural crops $\{A_i^k\}_{i \in S, k \neq K}$.[24] The underlying rationale is that the GAEZ data provides potential yields and is thus informative about the yield variation across location-crops that is driven exclusively by differences in natural characteristics, including the climate. The variation in effective yields across locations, conditional on the former, is embedded in $\{b_i^k\}_{i,k}$.

[24] To be consistent with the SSA rural context in 2000, I use the agro-climate potential yields calculated for rain-fed agriculture with low usage of modern inputs. See Appendix C.1 for details.

To quantify the remaining elements, I implement the following two-stage calibration algorithm. Starting with a guess for τ_{ij}^F, the first stage (inner loop) simultaneously solves for $\{A_i^K\}_i$, $\{b_i^k\}_k$, and $\{\Omega_a, \Omega_K\}$ by inverting the spatial equilibrium so that the model matches, respectively, the spatial distributions of GDP, the spatial distribution of sectoral production, and the relative a and K aggregate expenditure shares.

Importantly, my method identifies the product $\{b_i^K A_i^K\}_i$ (since its two elements cannot be separated), and pins down $\{b_i^k\}_{k \neq K}$ in relative terms within locations. Therefore, the latter is identified using within-crop variation in observed production across locations, conditional on the fundamental productivities of $\mathcal{A}$. The former, conditional on the latter, is identified using spatial variation in GDP.

The second stage (outer loop) is much simpler: it iterates the first stage over several values of τ_{ij}^F and pins down the one for which the model matches actual values of aggregate bilateral trade flows across countries. The calibrated $\tau_{ij}^F = 2.175$ is close to values from the literature, such as 1.15 from Baum-Snow et al. (2020) or 2.375 from Antràs et al. (2022).

5.4 Migration frictions and amenities

As with τ_{ij}, I set the bilateral component of migration frictions to be proportional to distance, i.e. $m_{ij} = \text{distance}(i,j)^\phi$. Thus, the remaining elements to be quantified are $\{\phi, m_c, u_i\}_{i,c}$, which are solved for with an analogous two-stage procedure.

The inner loop first uses the quantified elements in Section 5.3 to solve for prices (eqs. (21), (22) and (24)) and real wages in the economy. Then, starting with a guess for ϕ, it inverts the spatial equilibrium for $\{m_c\}_c$ and $\{u_i\}_i$ such that the model replicates, respectively, the gross migration flows at the country level and the spatial distribution of population.[25] The separate identification of $\{m_c\}_c$ and $\{u_i\}_i$ is possible because they are additively separable in the denominator of eq. (23). That provides within-country variation in terms of potential origins from which the migration cost is or is not scaled by $\{m_c\}_c$, and allows for a separate identification conditional on $\{u_i\}_i$.[26] The latter, conditional on the former, is identified with spatial variation in population.[27]

[25] Importantly, the migration data represent cross-country gross flows between 1990 and 2000. Thus, my estimation requires a measure of the initial population in 2000, i.e. $\{L_i^0\}_i$. I calculate it by scaling the distribution of the population in 1990 to the levels of SSA population in 2000, while accounting for the observed natural population growth rates (fertility minus mortality) across countries during the period. Intuitively, this represents the population distribution in SSA if there had been no mobility during that period.

[26] Intuitively, the additive separation holds because, for each destination, there are several origins of migrants, some of them being other countries and others not.

[27] Therefore, amenities stand as a structural residual of my model: it rationalizes all location choices observed in the data that cannot be explained by differences in real wages and migration frictions.

The outer loop consists of a similar grid search over ϕ. It iterates the inner loop for several values and chooses the one for which the model-generated internal migration matches the data. The value $\phi = 0.5$ is larger than comparable estimates from the literature, such as 0.06 for the US (Allen and Donaldson, 2022) and 0.35 for Brazil (Morten and Oliveira, 2018).[28] Yet, it squares with recent evidence in the literature that suggests an inverse relation between economic development and mobility frictions.[29]

5.5 Discussion of the results

Figure 5 illustrates the spatial distribution of some of the quantified fundamentals. Panel A and B show that more productive locations (which have higher real wages) have higher fundamental productivities in the K^{th} sector. Thus, the model rationalizes that, net of the variation in the $K-1$ sectors, locations with a high level of economic activity must be very productive in non-agriculture. This pattern stands out in some capitals and in high-GDP countries, such as South Africa. Panel C illustrates an analogous aspect of the quantified sectoral shifters of cassava. Thus, there are high $\{b_i^k\}_i$ values for locations in countries that are large cassava producers, such as Nigeria.

Moreover, Panel D and E show that high-amenity locations have relatively high population density and very low real wages. DR Congo and Zimbabwe are two examples. Their higher amenities are utility compensations that explain why individuals are not living somewhere else in SSA. Intuitively, this captures local cultural or institutional characteristics that work as pull factors (which will be kept constant in the counterfactuals).

However, these characteristics do not include migration frictions, since they are accounted for separately in my framework. To illustrate, Panel F plots the distribution of the quantified country-level migration barriers, i.e. $\{m_c\}_c$. High-barrier countries display two characteristics: higher income differentials relative to neighboring countries and relatively low inflows of migrants. The Central African Republic and South Africa (which are geographically close to DR Congo and Zimbabwe, respectively) illustrate this. Their relative income differences (with respect to their surrounding countries) are disproportionally larger than the observed total flow of immigrants, which implies higher migration barriers.[30]

[28] Note that Morten and Oliveira (2018) estimate an elasticity of bilateral migration flows with respect to bilateral travel distance of about -0.7. Through the lens of my model, this elasticity reads as $-\theta \times \phi$.

[29] Bryan and Morten (2019), for instance, estimate average mobility frictions in Indonesia that are three times higher than in the US.

[30] A second mechanism explaining the variation in country barriers is the absolute variation in migration flows. Countries with low migration flows, even if at the left of the real wage distribution, must have, at least to some extent, relatively high migration barriers. The reason for this is the idiosyncratic component of workers' preferences, which generates some migration that must somehow be rationalized.

Figure 5: Comparison between the calibrated fundamentals and the observed endogenous variables

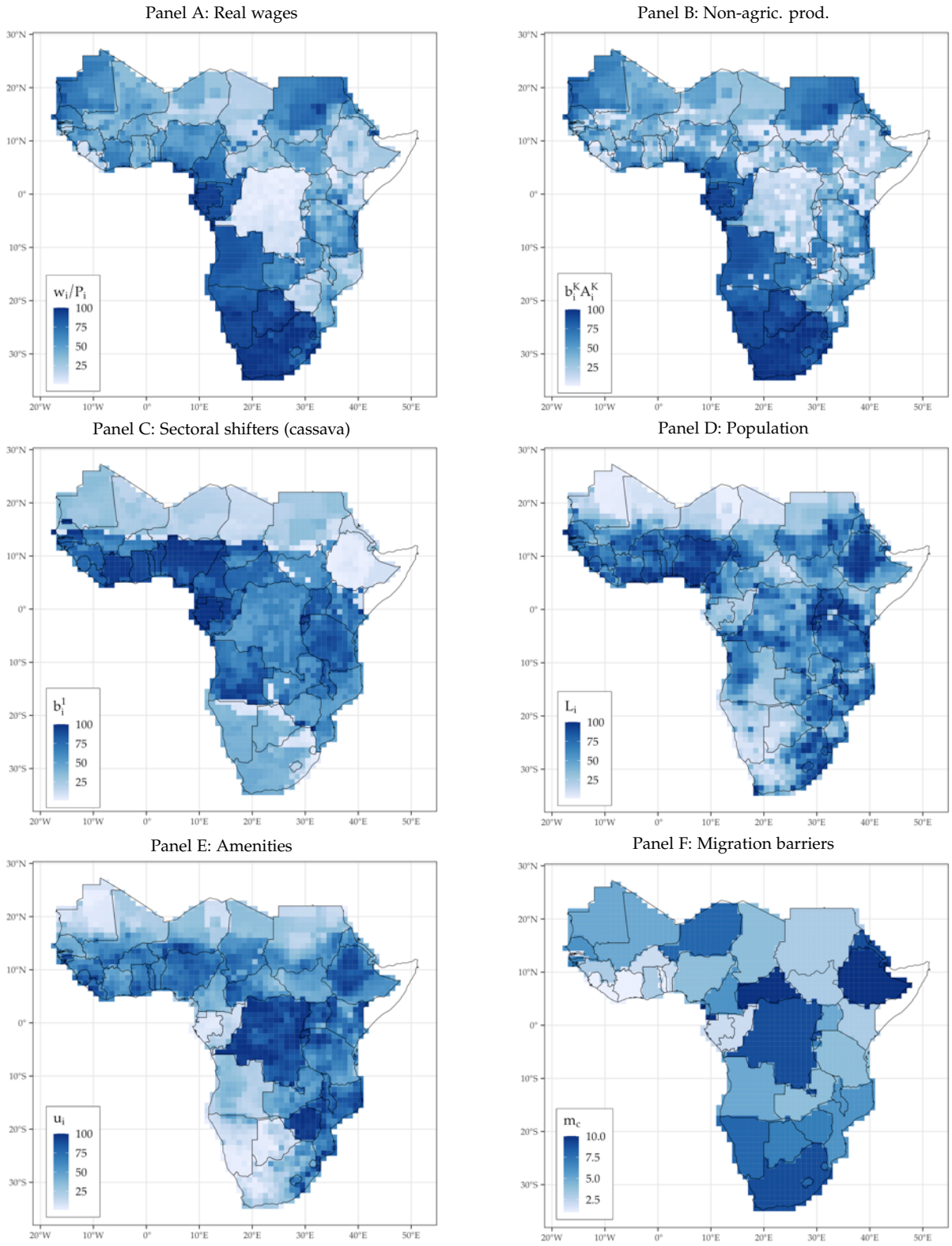

Notes: Each panel plots the spatial distribution of the quantified fundamentals as explained in sections 5.3 and 5.4. The results are shown in percentiles, where 1 and 100 stand for the bottom and top percentiles of each sample, respectively. Panel F documents results analogously, but in deciles.

5.6 Validating the model

Before using the calibrated model to simulate the future, I test its capacity to replicate observed moments. I start with a backcasting exercise that solves for the spatial equilibrium in 1975 using the GAEZ agricultural productivities and population endowments in that year. The result illustrates the extent to which the model is able to replicate the population changes in SSA between 1975 and 2000 using the observed changes in climate conditions during that period.[31]

Panels A and B of Figure 6 report the results in levels. The model closely replicates the spatial distribution of the population in 1975 both within and across countries. Moreover, Panel C shows that the results closely fit the population changes between 1975 and 2000, with a slope of 0.83 and $R^2 = 0.92$. Importantly, the major change in this backcasting exercise is on the agricultural suitabilities, i.e. $\{A_i^k\}_{i,k\neq K}$. According to the GAEZ estimates, about 75 percent of the locations in SSA experienced a decline in crop yields between 2000 and 1975. Thus, the fact that using this variation in the model can explain the changes in population during the period confirms the model's capacity to provide reliable forecasts of the future using the GAEZ estimates.[32]

As an additional overidentification test, in Panel D I compare country-level agricultural employment shares (for all crops) generated by the model for 2000 against World Bank data. The model closely replicates the ranking of countries with respect to agricultural employment shares, though it underestimates their levels. In aggregate, the model predicts about a 20 percent share of employment in agriculture as compared to 58 percent in the data. The main reason for this discrepancy is that I include only a subset of the crops produced in SSA.

6 Climate change and migration: the 2080 forecast

I quantify potential climate migration in SSA by performing a series of counterfactual simulations using the calibrated model. The benchmark exercise consists of solving for the spatial equilibrium in 2080 with and without climate change. By comparing the two, I am able to quantify the population reallocation driven by climate change.

[31] The data source for the 1975 population (GHSP) differs from that used in the calibration (G-Econ). I check their compatibility using the correlation between them for the population in 2000 (available in both datasets) at the grid-cell and country level. Furthermore, in order to have an initial population for solving the model for 1975 – i.e. $\{L_i^0\}_i$ – I project the 2000 population distribution onto the 1975 levels. Appendix A.7 discusses that in detail.

[32] A complementary explanation for the good fit in this exercise is path dependence (i.e. the densest locations in 1975 are also the densest in 2000). That is, in a context of high mobility frictions, such as in SSA, the geography of the economy needs extreme shocks to its fundamentals in order to generate dramatic changes in this kind of counterfactual. As shown in Figure A.2, the changes between 1975 and 2000 are not as dramatic as the ones expected by 2080.

Figure 6: Validation of the calibrated model in levels and differences

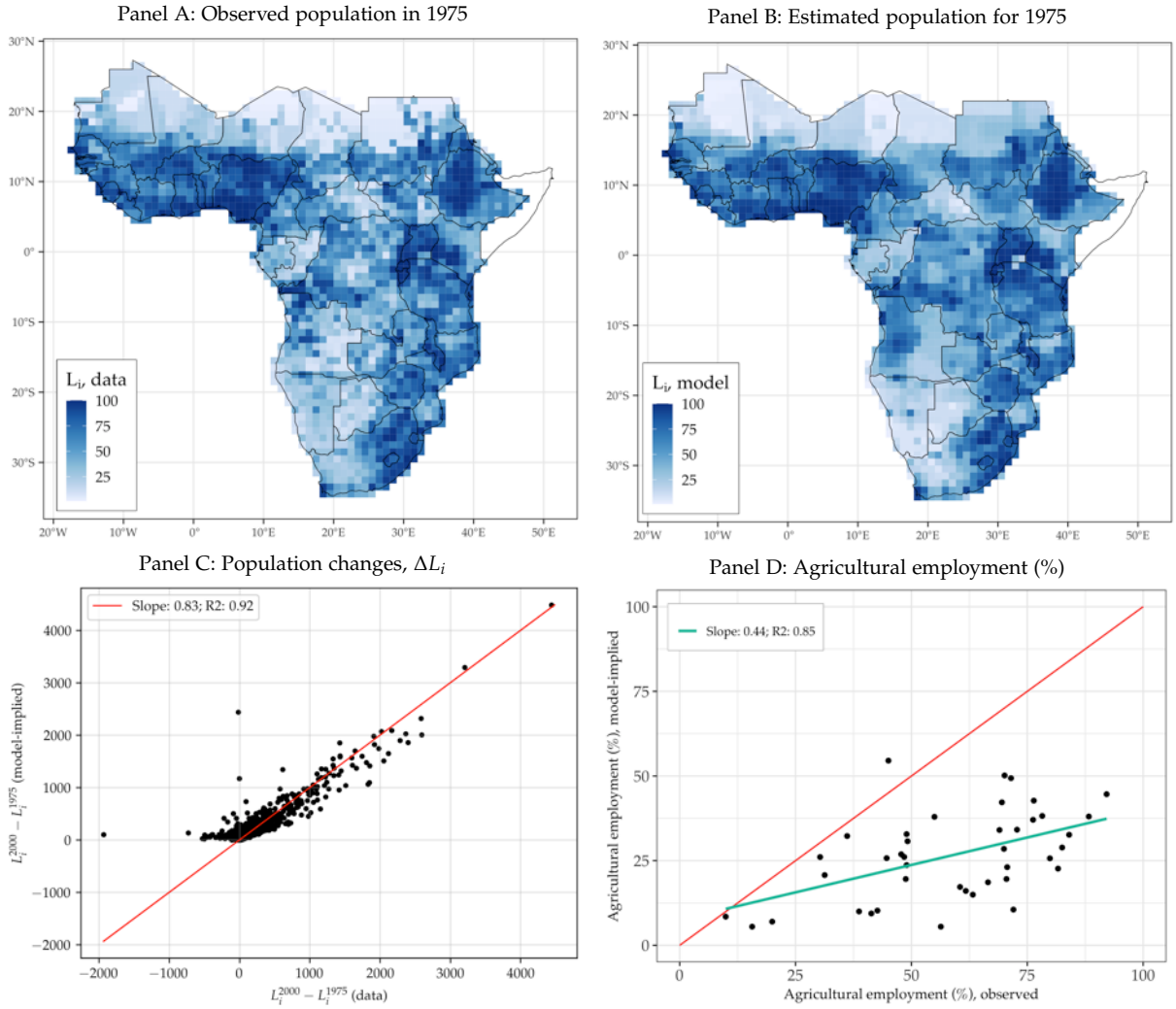

Notes: Panels A shows the observed 1975 population distribution in SSA while Panel B shows the distribution produced by the model. The values are shown in percentiles, where 1 (100) stands for the bottom (top) percentile of each sample. Panel C plots the model fit in terms of population change (between 1975 and 2000, in thousands) while Panel D plots the model fit for country-level agricultural employment in 2000 (in percentage points).

Subsequently, I study the role of the model's mechanisms and conduct a policy experiment that investigates the impact of climate change if SSA becomes as frictionless as the EU (in terms of migration and trade barriers). I conclude with robustness checks.

6.1 Benchmark counterfactual

I solve for the spatial equilibrium in 2080 by inserting the 2080 forecasts of the initial population $\mathcal{L}$ and crop productivities $\mathcal{A}$ into the calibrated model. The former is obtained by scaling the observed population of 2000 using the estimates of country-level population increase from the Population Prospects of United Nations and Social Af-

fairs (2019) for 2080.[33] The latter, in contrast, is taken directly from the GAEZ data. For the climate change simulations, I use the estimates of potential crop yields in 2080 based on the most extreme future scenario available. Hence, the benchmark climate change results represent an upper bound in terms of magnitudes since they reflect the most pessimistic future for SSA.[34] The simulations with no climate change assume no changes in $\mathcal{A}$ and thus capture only the increase in population $\mathcal{L}$.[35]

I quantify climate migration, ΔL_i, using the differences between the equilibrium populations of the two simulations – with and without climate change. Hence, it measures migration pressure in each location i net of the potential migration inflows and outflows. Similarly, I infer the changes in sectoral specialization from the differences in non-agricultural employment ΔL_i^K (in percentage points) and the welfare changes from the percentage change in real wages, $\Delta w_i / P_i$.

Figure 7 shows the results on a map. At the country level, Panel A shows large climate migration flows – on the order of half a million individuals or more – from the Western Sahel countries to nearby non-Sahel Western Africa (e.g. Liberia, Ivory Coast, Ghana, and Nigeria) and from DR Congo to Eastern Africa countries. Panel B, which presents grid-cell-level results, shows a high degree of within-country heterogeneity. Countries experiencing the largest migration outflows, such as Mali and DR Congo, also experience a high level of internal migration. There are large movements from their central and northern locations, which are highly affected by climate change, to their relatively less affected southern locations. Overall, countries heterogeneously hit by climate change experience large internal migration flows and large population increases in their capitals.[36]

Panels C to F show the results in terms of structural change and real GDP per capita. The countries that benefit from climate change, such as Tanzania, Rwanda, and Uganda, specialize into agriculture (Panel C). This occurs because such an increase in comparative advantage transforms them into the new agricultural powerhouses of SSA. As a consequence, their real wages increase (Panel E), which attracts

[33]These estimates project the observed country-level natural rates of population growth (fertility minus mortality without migration) at the beginning of the 21st century onto subsequent years. Hence, I assume that fertility is exogenous. Section 6.4 shows how the results change if fertility is endogenized.

[34]When drawing the GAEZ data for 2080, I chose the scenario that is closest to Representative Concentration Pathway (RCP) 8.5 (the standard for a severe and fuel-intense future; see Appendix C.1for details). I also smooth out positive outliers in the spatial aggregation by centering it on the bottom deciles within grid cells. As robustness, I check the sensitivity of the results to this aggregation method and to the choice of less severe future scenarios. As expected, assuming a less pessimist scenario reduces the magnitude of the climate change impact. See Section 6.4 and Appendix D.1 for details.

[35]Note that the spatial distribution of outcomes in the no-climate-change simulations differs from the observed distribution for 2000 due to dispersion forces driven by θ and α.

[36]See Table D.3 for details. Note that the large estimated increase in the populations of capital cities is consistent with the findings in the empirical literature on the high urbanization rates associated with climate change (e.g. Henderson et al., 2017; Peri and Sasahara, 2019; Castells-Quintana et al., 2021).

Figure 7: Counterfactual results for a climate-changed SSA in 2080

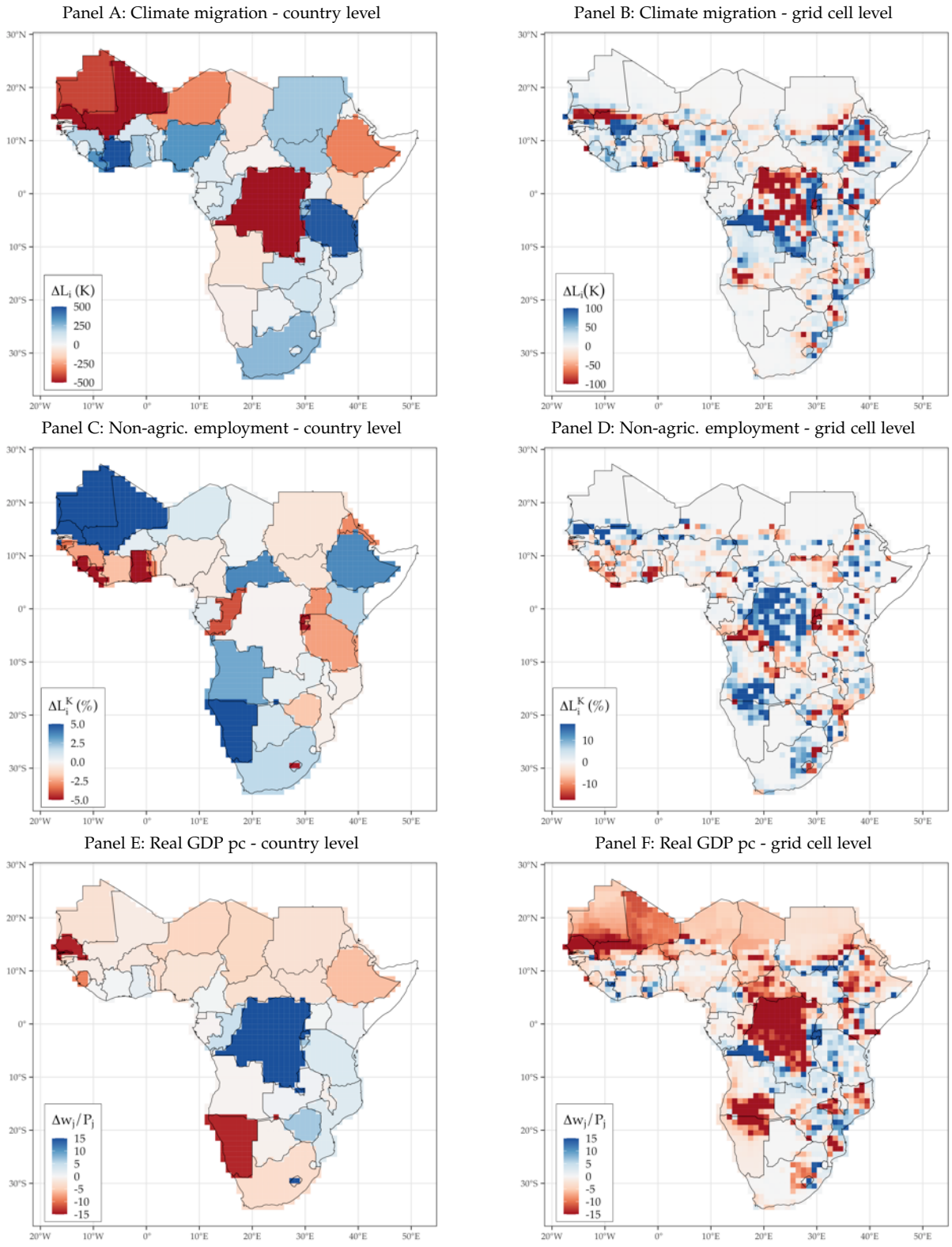

Notes: Panel A and B plot the results of climate migration in thousands of individuals. Panel C and D describe the results in terms of non-agricultural employment, in percentage points. Panel E and F present the welfare results in terms of percentage changes in real GDP per capita.

migrants from nearby countries, such as DR Congo, Kenya and Ethiopia. Panel D and F illustrate the richness of these results in terms of within-country heterogeneity. Even within countries that benefit from climate change, there is substantial variation in terms of sectoral specialization and welfare effects.

Nevertheless, some countries forcedly shift towards agriculture in a non welfare-improving way. Nigeria is an example: compared to the no climate change scenario, it needs to produce higher crop quantities to supply food to nearby countries that, being much more affected by climate change, specialize out of agriculture (e.g. Mali and Senegal). This shows that the necessity aspect of crops limits the Western African economies to adapt to climate change (through structural change) and force them into a climate change-driven poverty trap. Interestingly, the opposite holds for DR Congo. Climate change pushes individuals from its poorest regions either abroad or to its more productive south. As it stands among the poorest SSA countries in the no climate change scenario, such a productivity-improving reallocation drastically increases real wages in relative terms.

In aggregate, the estimated climate migration flows in SSA total about 4 million individuals (Panel A of Table 2 column 1). This is much lower than Rigaud et al. (2018)'s estimates of 90 million climate migrants in SSA by 2050. This discrepancy is explained by the migration frictions that I account for and estimate using actual migration data. Without them, my estimates of climate migration increase by more than 100 million individuals.[37] I explore this result in detail, together with other aspects of the role of migration barriers, in Sections 6.2 and 6.3.

Table 2 also shows that climate change reduces real GDP per capita by about 1.2 percent. Importantly, this seemingly small effect hides a large degree of heterogeneity. At the country level, the bottom and top deciles of changes in real GDP per capita are -6 percent and 6.5 percent, respectively (Panel B). Thus, the adaptation to climate change will lead to unequal consequences across SSA, generating winners and losers. This final outcome depends on several mechanisms that interact with each other, such as migration barriers and the heterogeneous forces driving sectoral specialization and structural change across countries. I investigate the welfare importance of these mechanisms in Section 6.2.

Furthermore, the overall negative impact of climate change on agricultural productivity reduces aggregate non-agricultural employment by 0.85 percentage points. This is because more labor now needs to be employed in agriculture in order to produce the necessary aggregate quantity of crops (which makes the economy poorer

[37]This pattern is consistent related findings that show that large mobility frictions in developing economies may have an inhibiting effect on future climate migration and thus may exacerbate welfare losses (e.g. Peri and Sasahara, 2019; Benveniste et al., 2020; Burzyński et al., 2022).

Table 2: Aggregate and disaggregate results of the climate change counterfactuals for 2080

	(1) Baseline	(2) No country barriers	(3) No migration frictions	(4) Higher trade costs	(5) Higher trade + low mig.
Panel A - Aggregate CΔ effects:					
Climate migration[1]	4.02	62.05	114.63	17.4	59.17
Δ GDP pc (%)	-1.18	3.65	9.23	-7.05	-3.40
ΔL_i^K (non–agric. employment, %)	-0.85	0.27	1.36	-3.19	-2.33
Panel B - Country–level CΔ effects:					
Median Δ Population[1]	0.03	0.03	-0.35	0.16	0.68
Bottom/top deciles	[-0.31; 0.25]	[-4.55; 2.63]	[-7.21; 7.32]	[-1.05; 1.53]	[-5.75; 3.14]
Median Δ GDP pc (%)	-0.72	1.2	-0.43	-2.32	-0.19
Bottom/top deciles	[-6.01; 6.53]	[-9.35; 19.62]	[-13.21; 49.59]	[-29.65; 17.82]	[-34.93; 42.45]
Median ΔL_i^K (%)	-0.31	0.71	1.72	-2.45	-1.83
Bottom/top deciles	[-7.57; 3.7]	[-3.66; 6.94]	[-4.64; 9.54]	[-11.3; 3.92]	[-8.59; 3.74]
Panel C - Gross migration with CΔ:					
Ratio: International/Internal migration flows	0.11	5.06	19.42	0.14	0.25

Notes: The results present the outcomes in 2080 for several counterfactual simulations of a climate-changed SSA. In particular, column 1 shows the baseline results, column 2 shows the results with no country migration barriers ($m_c = 1$ for all c), and column 3 shows the results with no bilateral migration barriers of any kind ($m_{ij} = 1$ for all i,j). Column 4 shows the results of the counterfactual with greater trade frictions (an increase of 50 percent in δ). Column 5 shows the results with greater trades friction and lower bilateral migration barriers (a decrease of 50 percent in ϕ). [1]Climate migration in million individuals.

and increases the agricultural expenditure share).[38] In distributional terms, however, this effect is heterogeneous and negatively skewed: the top and bottom deciles of the country-level changes in non-agricultural employment are -7.5 percentage points and 3.7 percentage points, respectively.

Finally, Panel C shows that the aggregate gross internal migration flows in the climate change scenario are almost ten-fold larger than the international migration flows. This suggests that the country migration barriers $\{m_c\}_c$ are playing a central role in individuals' migration decisions in response to climate change. In what follows, I investigate the importance of these barriers relative to the bilateral component of mobility frictions, as well as the role of several other underlying mechanisms driving the results presented so far.

[38]This result is consistent with related findings in the literature. For instance, Nath (2022) estimates an increase in agricultural expenditure shares of about 2.7 percentage points in the world's poorest quartile of countries, whereas Cruz (2021) estimates an increase in global agricultural employment of about 2 percent. The main channel explaining the differences in magnitude between those estimates and my own (0.85) is the multi-crop feature of my framework. By not taking into consideration the potential production reallocation within agriculture (i.e. across crops), the consumption specialization effect of climate change is overestimated. I discuss this extensively in Section 6.2.

6.2 Investigating the underlying channels

I investigate the extent to which the model's underlying channels (migration frictions, trade, and crop-switching) affect the estimated climate migration flows and the associated welfare and sectoral specialization effects. To do so, I perform additional simulations centered on each of the channels and highlight how they interact with one another.

Migration frictions. I start with the role of country migration barriers $\{m_c\}_c$. Column 2 of Table 2 summarizes the results of a counterfactual in which country barriers are eliminated (i.e. $m_c = 1$ for all c).[39] As expected, aggregate migration flows increase substantially – by almost 60 million climate migrants. Perhaps surprisingly, the welfare losses associated with climate change are fully reversed: real GDP per capita in SSA increases by 3.65 percent. These patterns are further amplified in the counterfactual that eliminates bilateral mobility frictions completely (i.e. $\bar{m}_{ij} = 1$ for all i,j; results appear in column 3). In that case, climate migration flows increase by about 110 million individuals and real GDP per capita increases by 9.23 percent.

What explains this welfare-improving role of migration as adaptation? The answer lies in its interaction with sectoral specialization. In the absence of mobility frictions, workers in affected areas can migrate to farther-away, more productive regions, which improves the efficiency of the SSA economy in terms of sectoral comparative advantage. In the climate change scenario, this means that agricultural production reallocates to the climate-change-benefitted regions, while non-agricultural production moves to the most developed countries in SSA. This efficiency gain increases real income in SSA, which reduces the demand for agricultural goods and employment in that sector. Thus, migration allows SSA to benefit from the push-aspect of climate change by permitting individuals to move out of unproductive rural regions and allowing the economy to go through a welfare-improving process of structural transformation.

Table 2 Panel B provides quantitative evidence of this result. The distribution of non-agricultural employment changes across countries shifts rightwards when mobility frictions are reduced, thus confirming that more countries specialize out of agriculture in this scenario. Table 3 presents results for selected countries. Reducing mobility frictions intensifies the welfare losses in the most affected countries (such as Senegal) and the previously discussed patterns in DR Congo and Nigeria. Their non-agricultural employment increases because benefitted countries, such as Tanzania,

[39] In particular, this counterfactual assumes no country barriers in the simulations with and without climate change. Thus, the comparison of the two isolates the climate change effect and shows how they compare with the baseline in the absence of these barriers. The same applies to the counterfactuals below.

Table 3: Results of selected climate change counterfactuals for selected countries

	(1) Senegal	(2) DR Congo	(3) Nigeria	(4) Tanzania	(5) South Africa
Panel A - Baseline results:					
Δ Population[1]	-0.58	-1.20	0.34	0.48	0.25
Δ GDP pc (%)	-14.07	20.00	-2.58	2.77	-3.43
Δ Non-agric. employm. (%)	8.10	-0.10	-0.44	-2.53	1.78
Panel B - No country migration barriers:					
Δ Population[1]	-5.11	-21.97	-0.31	6.57	10.12
Δ GDP pc (%)	-14.15	43.01	-2.59	4.86	2.89
Δ Non-agric. employm. (%)	8.87	2.47	0.67	-3.41	3.09
Panel C - No migration frictions:					
Δ Population[1]	-5.62	-32.05	-6.79	16.59	9.98
Δ GDP pc (%)	-23.93	49.59	-3.45	11.21	3.90
Δ Non-agric. employm. (%)	9.54	4.85	1.23	-6.89	5.09

Notes: Panel A documents the results of the baseline counterfactual (column 1 of Table 2) for selected countries. Panel B and C present the results for the same countries for the counterfactuals corresponding to columns 2 and 3 of Table 2. [1]Climate migration in million individuals.

shift even more into crop production and become the destination for larger climate migration inflows. In fact, this also permits developed countries like South Africa to further specialize in non-agriculture (by outsourcing crops), to attract additional climate migrants, and to overcome the welfare losses from climate change.

Importantly, these aggregate gains hide an increase in inequality across countries. Columns 2 and 3 of Table 2 Panel B show that the distribution of changes in real GDP per capita widens as migration frictions are reduced. That is, migration allows SSA to adapt to climate change in an aggregate welfare-improving manner, although it makes the individuals remaining in the most-affected regions worse off.[40] Therefore, the results imply that mitigating climate change by reducing migration barriers poses a trade-off between aggregate gains and increasing inequality. In Section 6.3, I explore this in detail and show that trade policy can attenuate this trade-off.

The role of trade. Table 2 Column 4 presents the results of a counterfactual with higher trade frictions (i.e. increasing δ by 50 percent). On aggregate, climate migration flows and welfare losses increase dramatically, by about four-fold and seven-fold, respectively. This occurs because greater trade friction inhibits the ability of the economy to adapt through sectoral specialization, thus incentivizing migration

[40]Note that eliminating migration frictions $\bar{m}_{ij}$ completely does not remove the congestion forces in the economy. The heterogeneity of agents with respect to their location choice (disciplined by θ and α) still works as a dispersion force, thus preventing all agents from moving to the best locations in the economy.

(as in Conte et al., 2021). Moreover, higher trade friction intensifies the food problem: aggregate agricultural employment increases and the country-level distribution of non-agricultural employment shifts leftwards. This is consistent with the theoretical insights in Section 4.3 and shows that trade has a crucial adaptive role, disciplining both climate migration and welfare losses in SSA.

Next, I investigate how that effect interacts with migration in another simulation that, on top of the higher trade frictions, reduces migration barriers (i.e. reducing ϕ by 50 percent; results in column 5). Climate migration flows triples, welfare losses decrease by half, and agricultural employment decrease by one third. That emphasizes, once again, that migration as adaptation can be welfare-improving, on aggregate, by allowing for structural change at the cost of increasing inequality.

Crop switching. To investigate the importance of the multi-crop feature of my framework, I perform a counterfactual exercise in which agriculture is comprised of a single crop (results in Table 4 column 2).[41] Compared to the baseline, climate migration decreases only slightly. However, welfare losses and non-agricultural employment increase dramatically. This is explained by the heterogeneity of the expected crop yield changes within locations (Figure 1). Affected producers can, in the multi-crop model, reallocate agricultural production to the less-affected crop (but not in the case of a single crop). Hence, assuming a single crop overestimates the impact of climate change on agricultural productivity and amplifies the necessity for the economy to allocate, on aggregate, more labor into agriculture.[42] Thus, accounting for this margin is key in correctly predicting the impact of climate change on agriculture and the resulting effects in subsistence rural economies like those in SSA.

6.3 Policy experiment - SSA as frictionless as the EU

One of the key takeaways from Section 6.2 is the tradeoff that migration policy poses: it allows SSA to be better-off when adapting to climate change at the expense of higher regional inequality. Hence, a question that naturally emerges is whether other policy tools can attenuate this tradeoff. In what follows, I focus on trade policy. In particular, I conduct a policy experiment that quantifies the consequences of climate change for SSA in the hypothetical scenario where migration and trade frictions are reduced to the levels prevailing in the EU.

Doing so requires the quantification of the migration and trade frictions in the EU within the structure of the model. I do that by mapping the country migration

[41] I assume a representative crop whose spatial distribution of potential yields is the cross-crop average within a location. See Appendix B.1 for details.

[42] In fact, assuming a single crop brings my sectoral specialization results much closer to the findings of related studies that assume the same structure (e.g. Cruz, 2021; Nath, 2022, see footnote 38).

Table 4: Aggregate and disaggregate results of the climate change counterfactuals and policy experiments for 2080

	(1) Baseline	(2) Agriculture as one crop	(3) EU trade frictions	(4) EU mig. barriers	(5) EU trade + mig. barriers
Panel A - Aggregate CΔ effects:					
Climate migration[1]	4.02	3.23	2.78	29.14	21.08
Δ GDP pc (%)	-1.18	-3.48	-0.31	0.03	0.54
ΔL_i^K (non–agric. employment, %)	-0.85	-2.73	0.33	-0.64	0.64
Panel B - Country–level CΔ effects:					
Median Δ Population[1]	0.03	0.01	0.02	0.11	0.09
Bottom/top deciles	[-0.31; 0.25]	[-0.27; 0.25]	[-0.31; 0.25]	[-2.83; 1.56]	[-1.47; 1.16]
Median Δ GDP pc (%)	-0.72	-4.42	-0.09	-0.12	-0.01
Bottom/top deciles	[-6.01; 6.53]	[-10.45; 1.27]	[-2.97; 1.68]	[-7.02; 12.36]	[-2.76; 5.4]
Median ΔL_i^K (%)	-0.31	-1.95	0.03	0	0.1
Bottom/top deciles	[-7.57; 3.7]	[-7.04; 1.78]	[-4.38; 6.92]	[-7.08; 4.84]	[-5.35; 8.16]
Panel C - Gross migration with CΔ:					
Ratio: International/Internal migration flows	0.11	0.11	0.11	1.21	1.38

Notes: The results relate to several counterfactual simulations of a climate-changed SSA in 2080. In particular, column 1 corresponds to the baseline results, while column 2 presents the results when assuming a single crop. Columns 3 to 5 present the results of policy experiments in which frictions are equated to EU levels: in column 3, SSA adopts the same level of tariffs as the EU; in column 4 it adopts the same migration policy, and in column 5 it combines both policies. [1]Climate migration in million individuals.

barriers $\{m_c\}_c$ and the tariff component of trade frictions τ_{ij}^F to EU migration and trade policies. Focusing on these parameters is particularly convenient because they reflect the institutional characteristics of the EU in terms of trade and migration policies. In other words, they are more tangible – being policy tools – than the elasticity parameters ϕ or δ.[43]

In practice, I quantify $\{m_c\}_c$ and τ_{ij}^F by bringing the model to the EU data using the procedure described in Section 5.[44] The estimated EU frictions are substantially lower than those in the SSA. With respect to trade, I estimate $\tau_{ij}^F = 0.025$, which is almost a hundred-fold less than in SSA. This is shown in Figure 8 Panel A, where the discontinuity in bilateral frictions for cross-country trade is barely visible. It also shows that the estimated EU country migration barriers are much less stringent. The average $\{m_c\}_c$ is 35 percent lower than in the SSA case, and its distribution is shifted

[43]Moreover, a comparison to the EU provides results that are more policy-relevant: equating the parameters to EU levels reflects tangible policy actions with a real-world connection. This is less the case with arbitrary changes, as in Section 6.2.

[44]This requires data for the same period and therefore the estimated values for the EU are also for 2000. Importantly, I focus on isolating the variation in the observed trade and migration flows within the EU. Thus, the values of the preference parameters and the bilateral elasticities δ and ϕ remain as described in Table 1. See Appendix A.8 for details.

Figure 8: Estimated trade and migration frictions in the European Union

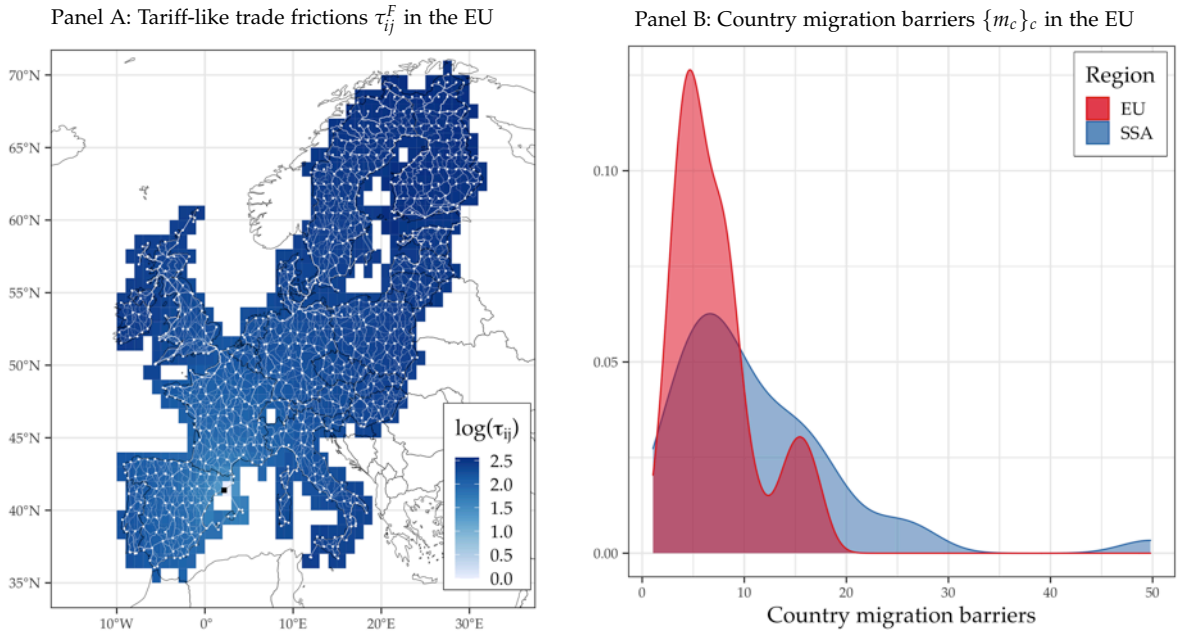

Notes: Panel A presents trade frictions in the EU as was done for SSA in Figure 4 (in this context, trade frictions are relative to Barcelona (Spain), represented by the black dot). Panel B plots the distribution of country migration barriers $\{m_c\}_c$ in SSA and the EU.

far more to the left (Panel B).

Armed with that, I perform counterfactual simulations that replace the trade and migration barriers with the EU values. Table 4 Column 3 shows the results for trade policy only. Reducing tariffs to EU levels reduces climate migration flows by almost half, attenuates aggregate losses, and slightly shifts the economy out of agriculture. As in Section 6.2 (though, in this case, in the opposite direction of Table 2 Column 4), the underlying channel is the higher adaptive capacity achieved through sectoral specialization. Thus, trade policy can be a powerful tool for a policy maker interested in reducing migration flows and attenuating the aggregate and distributional impacts of climate change.

I next conduct an analogous exercise that instead reduces country migration barriers to EU levels (column 4).[45] In line with previous results, there is an increase in climate migration (Panel A), and primarily between countries (Panel C), which sets off the migration-induced process of structural change described in Section 6.2. The magnitude of the results is not as stark as in that case. Nonetheless, they do show that by reducing country migration barriers to EU levels, a policy maker in SSA can eliminate the aggregate losses due to climate change, although at the cost – as before – of an increase in climate migration and regional inequality.

[45] I match the EU $\{m_c\}_c$ values to the SSA countries by deciles (i.e. scaling the barriers of the SSA countries to the value of their respective decile in the EU distribution). See Appendix A.8 for details.

Finally, I combine both policies (column 5) and find that trade policy drastically attenuates the inequality effect of the migration policy. In particular, Panel B shows a narrowing of the differences in welfare consequences between the most- and least-affected countries. The policy mix also increases the efficiency of the SSA economy, actually converting the aggregate losses into gains, and boosts the structural change process driven by migration. The importance of this policy experiment cannot be overstated: by combining both tools, a policy maker can take advantage of climate change by enabling SSA to reorganize more efficiently through trade and migration.

6.4 Robustness checks

In what follows, I check the robustness of the previous results in several dimensions: the friction parameters (trade and migration), the model's assumptions, and the climate change data used in the simulations. Table 5 below documents the main results, while Appendix B provides further details of the alternative models.

Friction parameters. Panel A illustrates the sensitivity of the benchmark results to changes in the friction parameters (i.e. increasing or decreasing ϕ or δ by 50 percent). The changes in the results are consistent with previous findings: trade frictions limit the capacity of the economy to adapt through sectoral specialization, and migration barriers prevent individuals from leaving affected locations, thus increasing losses.

Homothetic preferences. I now show that the nonhomotheticity feature of the preferences for agricultural goods and non-agricultural goods is a key driver of climate change's welfare consequences. Panel B shows the results of a counterfactual which assumes homothetic preferences (see Appendix B.2 for details). The aggregate flows of climate migration are not overly affected, but the welfare losses are dramatically reversed. This occurs because, by disregarding the subsistence aspect of agricultural goods, agents replace agricultural goods with non-agricultural goods. This intensifies the patterns of sectoral specialization (i.e. more production and consumption of non-agricultural goods takes place in the most affected regions). The opposite holds for the benefitted regions, which absorb most of the climate migrants and shift almost completely into agriculture (increasing aggregate agricultural employment).

Endogenous fertility. I perform a simple exercise that illustrates how the results change if fertility is allowed to be endogenous to climate change. To do so, I adjust the estimates for population growth taken from the Population Prospects of United Nations and Social Affairs (2019) using a damage function that depends on the average change in potential crop yields.[46] This reduces the initial population $\mathcal{L}$ assumed in the

[46] In particular, I assume that the rate of net population growth changes by 50 percent of the change

Table 5: Robustness of the benchmark results with respect to trade and migration frictions, model assumptions, and climate change scenarios

	(1) Climate migration (million individuals)	(2) Δ GDP per capita (%)	(3) Δ Non–agricultural employment (%)
Benchmark results	4.02	-1.18	-0.85
Panel A: Robustness to frictions			
Higher trade frictions	17.41	-7.05	-3.19
Lower trade frictions	2.01	0.10	0.50
Higher migration frictions	0.37	-1.78	-1.11
Lower migration frictions	24.47	1.06	-0.33
Panel B: Robustness to assumptions and CΔ scenario			
Homothetic preferences	3.52	4.38	-1.94
Endogenous fertility	2.52	2.72	1.77
RCP 4.5 scenario	1.34	1.86	1.28

Notes: Panel A presents the aggregate effect of climate change for different levels of trade and migration frictions, driven by the parameters δ and ϕ, respectively. Panel B presents the results of the benchmark simulation when (separately) assuming homothetic preferences between agriculture and non-agriculture, endogenous fertility, and a less severe climate change scenario.

counterfactuals for 2080, and particularly in the most-affected countries. This in turn reduces the potential number of climate migrants, as can be seen in Panel B. Moreover, endogenizing fertility results in an improved initial population distribution in 2080 (i.e. relatively higher initial populations in less-affected locations). This reduces the need for workers to migrate to the better-off locations in the economy and indeed reverses the aggregate welfare losses due to climate change.

Assumption of climate change scenario. I also check the sensitivity of the results to the severity of the underlying climate change scenario, by switching to the RCP 4.5 scenario (which assumes that carbon emissions will peak by mid-century and decrease thereafter). I simulate the model with the suitability data for this scenario (see Panel B of Table 5). As expected, climate migration is attenuated. Moreover, the results in terms of welfare losses and sectoral specializations are reversed. This occurs because the RCP 4.5 scenario reduces the losses from climate change more than the gains, which broadens the ability of the SSA to adapt through structural change.

in average potential yield in each location. Appendix B.3 provides further details and documents additional results with alternative scaling rules. Importantly, I adopt this approach for simplicity, rather than the more elaborate approaches in the literature (Delventhal et al., 2018, 2021; Cruz and Rossi-Hansberg, 2021), due to the static feature of my model.

7 Conclusion

The main message of this paper is that climate change must not lead to bad outcomes if rural economies like SSA can adapt to it. If mobility barriers can be reduced, climate change can encourage the shift of population out of poor, low-productivity rural locations and set off a process of structural change. Openness to trade determines the aggregate and distributional welfare effects of this process, by allowing affected economies to switch production to less-affected sectors. The interaction of these – and other – mechanisms in general equilibrium is complex and interconnected. I nevertheless model that with a transparent framework that I develop and connect to SSA data for 2000.

I identify that frictions in SSA are remarkably high and inhibit the welfare-improving process just described. My estimates suggest sizeable welfare losses of climate change and migration flows in many orders of magnitude smaller than reduced-form estimates from the literature. However, a policy experiment shows that, by becoming as frictionless as the EU, SSA adaptation to climate change could increase welfare both in aggregate and distributional terms. My climate migration estimates when relaxing migration frictions approach those from other studies that disregard these barriers.

My results deliver important contributions to the literature and the policy debates. I connect the findings from the literature on the gains from incentivizing migration in developing economies with those from the literature on the importance of sectoral specialization and trade in adapting to climate change. I also deliver a policy-relevant message on the potential role of real-world trade and migration policies in adapting to climate change.

References

Abel, Guy J and Joel E Cohen, "Bilateral international migration flow estimates for 200 countries," *Scientific data*, 2019, *6* (1), 1–13.

Albert, Christoph, Paula Bustos, and Jacopo Ponticelli, "The Effects of Climate Change on Labor and Capital Reallocation," Technical Report, National Bureau of Economic Research 2021.

Allen, Treb, "Information frictions in trade," *Econometrica*, 2014, *82* (6), 2041–2083.

_ **and Costas Arkolakis**, "Trade and the Topography of the Spatial Economy," *The Quarterly Journal of Economics*, 2014, *129* (3), 1085–1140.

_ **and Dave Donaldson**, "Persistence and path dependence in the spatial economy," 2022.

Antràs, Pol, Teresa C Fort, Agustín Gutiérrez, and Felix Tintelnot, "Trade Policy and Global Sourcing: An Efficiency Rationale for Tariff Escalation," Working Paper 30225, National Bureau of Economic Research July 2022.

Asturias, Jose, Manuel García-Santana, and Roberto Ramos, "Competition and the welfare gains from transportation infrastructure: Evidence from the Golden Quadrilateral of India," *Journal of the European Economic Association*, 2019, *17* (6), 1881–1940.

Atkin, David and Dave Donaldson, "Who's getting globalized? The size and implications of intra-national trade costs," Technical Report, National Bureau of Economic Research 2015.

_ **, Arnaud Costinot, and Masao Fukui**, "Globalization and the Ladder of Development: Pushed to the Top or Held at the Bottom?," Technical Report, National Bureau of Economic Research 2021.

Baez, Javier, German Caruso, Valerie Mueller, and Chiyu Niu, "Heat Exposure and Youth Migration in Central America and the Caribbean," *American Economic Review*, 2017, *107* (5), 446–50.

Balboni, Clare Alexandra, "In Harm's Way? Infrastructure Investments and the Persistence of Coastal Cities," 2021.

Barrios, Salvador, Luisito Bertinelli, and Eric Strobl, "Climatic change and rural–urban migration: The case of sub-Saharan Africa," *Journal of Urban Economics*, 2006, *60* (3), 357–371.

Baum-Snow, Nathaniel, J Vernon Henderson, Matthew A Turner, Qinghua Zhang, and Loren Brandt, "Does investment in national highways help or hurt hinterland city growth?," *Journal of Urban Economics*, 2020, *115*, 103124.

Benveniste, Hélène, Michael Oppenheimer, and Marc Fleurbaey, "Effect of border policy on exposure and vulnerability to climate change," *Proceedings of the National Academy of Sciences*, 2020, *117* (43), 26692–26702.

Borchert, Ingo, Mario Larch, Serge Shikher, and Yoto V Yotov, "The international trade and production database for estimation (ITPD-E)," *International Economics*, 2021, *166*, 140–166.

Brown, Oli et al., "Climate change and forced migration: Observations, projections and implications," Technical Report, Human Development Report Office (HDRO), United Nations Development Programme ... 2007.

Bryan, Gharad and Melanie Morten, "The aggregate productivity effects of internal migration: Evidence from Indonesia," *Journal of Political Economy*, 2019, *127* (5), 2229–2268.

Burzyński, Michał, Christoph Deuster, Frédéric Docquier, and Jaime De Melo, "Climate Change, Inequality, and Human Migration," *Journal of the European Economic Association*, 2022, *20* (3), 1145–1197.

Cai, Ruohong, Shuaizhang Feng, Michael Oppenheimer, and Mariola Pytlikova, "Climate variability and international migration: The importance of the agricultural linkage," *Journal of Environmental Economics and Management*, 2016, *79*, 135–151.

Caliendo, Lorenzo and Fernando Parro, "Estimates of the Trade and Welfare Effects of NAFTA," *The Review of Economic Studies*, 2015, *82* (1), 1–44.

_ , Luca David Opromolla, Fernando Parro, and Alessandro Sforza, "Goods and factor market integration: a quantitative assessment of the EU enlargement," *Journal of Political Economy*, 2021, *129* (12), 3491–3545.

Castells-Quintana, David, Melanie Krause, and Thomas KJ McDermott, "The urbanising force of global warming: the role of climate change in the spatial distribution of population," *Journal of Economic Geography*, 2021, *21* (4), 531–556.

CIESIN, "Global roads open access data set, version 1 (gROADSv1)," *Palisades, NY: NASA Socioeconomic Data and Applications Center (SEDAC)*, 2013.

Comin, Diego, Danial Lashkari, and Martí Mestieri, "Structural change with long-run income and price effects," *Econometrica*, 2021, *89* (1), 311–374.

Conte, Bruno, Klaus Desmet, Dávid Krisztián Nagy, and Esteban Rossi-Hansberg, "Local sectoral specialization in a warming world," *Journal of Economic Geography*, 2021, *21* (4), 493–530.

Costinot, Arnaud, Dave Donaldson, and Cory Smith, "Evolving comparative advantage and the impact of climate change in agricultural markets: Evidence from 1.7 million fields around the world," *Journal of Political Economy*, 2016, *124* (1), 205–248.

Cruz, Jose Luis, "Global Warming and Labor Market Reallocation," 2021.

Cruz, José Luis and Esteban Rossi-Hansberg, "The Economic Geography of Global Warming," Working Paper 28466, National Bureau of Economic Research February 2021.

Delventhal, Matthew J et al., "The globe as a network: Geography and the origins of the world income distribution," Technical Report, Mimeo, Claremont McKenna College 2018.

_ , Jesús Fernández-Villaverde, and Nezih Guner, "Demographic transitions across time and space," Technical Report, National Bureau of Economic Research 2021.

Desmet, Klaus and Esteban Rossi-Hansberg, "Spatial Development," *The American Economic Review*, 2014, *104*, 1211–1243.

_ and _ , "On the spatial economic impact of global warming," *Journal of Urban Economics*, 2015, *88*, 16–37.

_ , Dávid Krisztián Nagy, and Esteban Rossi-Hansberg, "The geography of development," *Journal of Political Economy*, 2018, *126* (3), 903–983.

_ , Robert E. Kopp, Scott A. Kulp, Dávid Krisztián Nagy, Michael Oppenheimer, Esteban Rossi-Hansberg, and Benjamin H. Strauss, "Evaluating the Economic Cost of Coastal Flooding," *American Economic Journal: Macroeconomics*, April 2021, *13* (2), 444–86.

Donaldson, Dave, "Railroads of the Raj: Estimating the impact of transportation infrastructure," *American Economic Review*, 2018, *108* (4-5), 899–934.

_ and Richard Hornbeck, "Railroads and American economic growth: A "market access" approach," *The Quarterly Journal of Economics*, 2016, *131* (2), 799–858.

Duarte, Margarida and Diego Restuccia, "The Role of the Structural Transformation in Aggregate Productivity," *Quarterly Journal of Economics*, 2010, *125* (1), 129–173.

Ducruet, César, Réka Juhász, Dávid Krisztián Nagy, and Claudia Steinwender, "All aboard: The effects of port development," Technical Report, National Bureau of Economic Research 2020.

Eaton, Jonathan and Samuel Kortum, "Technology, geography, and trade," *Econometrica*, 2002, *70* (5), 1741–1779.

Eckert, Fabian and Michael Peters, "Spatial structural change," *Unpublished Manuscript*, 2018.

Fajgelbaum, Pablo and Stephen J Redding, "Trade, Structural Transformation, and Development: Evidence from Argentina 1869–1914," *Journal of Political Economy*, 2022, *130* (5), 1249–1318.

Fan, Tianyu, Michael Peters, and Fabrizio Zilibotti, "Service-led or service-biased growth? Equilibrium development accounting across Indian Districts," Technical Report, National Bureau of Economic Research 2021.

Florczyk, AJ, C Corbane, D Ehrlich, S Freire, T Kemper, L Maffenini, M Melchiorri, M Pesaresi, P Politis, M Schiavina et al., "GHSL Data Package 2019," *Luxembourg. EUR*, 2019, *29788.*

Gemenne, François, Caroline Zickgraf, Elodie Hut, and Tatiana Castillo Betancourt, "Forced displacement related to the impacts of climate change and disasters," *9780198786467*, 2022.

Gollin, Douglas, Stephen L Parente, and Richard Rogerson, "The food problem and the evolution of international income levels," *Journal of Monetary Economics*, 2007, *54* (4), 1230–1255.

Gröger, André and Yanos Zylberberg, "Internal labor migration as a shock coping strategy: Evidence from a typhoon," *American Economic Journal: Applied Economics*, 2016, *8* (2), 123–53.

Henderson, J Vernon, Adam Storeygard, and Uwe Deichmann, "Has climate change driven urbanization in Africa?," *Journal of development economics*, 2017, *124*, 60–82.

Herrendorf, Berthold, Richard Rogerson, and Akos Valentinyi, "Growth and structural transformation," *Handbook of economic growth*, 2014, *2*, 855–941.

IIASA and FAO, "Global Agro-Ecological Zones (GAEZ v3. 0)," 2012.

IPCC, "IPCC Special Report," 2000.

_ , *Managing the risks of extreme events and disasters to advance climate change adaptation: special report of the intergovernmental panel on climate change*, Cambridge University Press, 2012.

Lagakos, David, Ahmed Mushfiq Mobarak, and Michael E Waugh, "The welfare effects of encouraging rural-urban migration," Technical Report, National Bureau of Economic Research 2018.

Lustgarten, Abrahm, "The Great Climate Migration Has Begun," *The New York Times*, Jun 2020.

Moneke, Niclas, "Can big push infrastructure unlock development? evidence from ethiopia," *STEG Theme*, 2020, *3*, 14–15.

Monte, Ferdinando, Stephen J Redding, and Esteban Rossi-Hansberg, "Commuting, migration, and local employment elasticities," *American Economic Review*, 2018, *108* (12), 3855–90.

Morten, Melanie and Jaqueline Oliveira, "The effects of roads on trade and migration: Evidence from a planned capital city," *NBER Working Paper*, 2018, *22158*, 1–64.

Myers, Norman, "Environmental refugees in a globally warmed world," *Bioscience*, 1993, *43* (11), 752–761.

_ , "Environmental refugees," *Population and environment*, 1997, *19* (2), 167–182.

_ , "Environmental refugees: a growing phenomenon of the 21st century," *Philosophical Transactions of the Royal Society of London. Series B: Biological Sciences*, 2002, *357* (1420), 609–613.

Nagy, Dávid Krisztián, "Hinterlands, city formation and growth: evidence from the US westward expansion," Technical Report 2022.

Nath, Ishan B, "The Food Problem and the Aggregate Productivity Consequences of Climate Change," Technical Report 2022.

Nordhaus, William, Qazi Azam, David Corderi, Kyle Hood, Nadejda Makarova Victor, Mukhtar Mohammed, Alexandra Miltner, and Jyldyz Weiss, "The G-Econ database on gridded output: methods and data," *Yale University, New Haven*, 2006, *6*.

of Economic United Nations, Department and Population Division Social Affairs, "World Population Prospects 2019: Highlights," 2019.

Pellegrina, Heitor S, "Trade, productivity, and the spatial organization of agriculture: Evidence from Brazil," *Journal of Development Economics*, 2022, p. 102816.

_ **and Sebastian Sotelo**, "Migration, Specialization, and Trade: Evidence from Brazil's March to the West," Technical Report, National Bureau of Economic Research 2021.

Peri, Giovanni and Akira Sasahara, "The impact of global warming on rural-Urban migrations: Evidence from global big data," Technical Report, National Bureau of Economic Research 2019.

Porteous, Obie, "High trade costs and their consequences: An estimated dynamic model of African agricultural storage and trade," *American Economic Journal: Applied Economics*, 2019, *11* (4), 327–66.

Redding, Stephen J, "Goods trade, factor mobility and welfare," *Journal of International Economics*, 2016, *101*, 148–167.

_ **and Esteban Rossi-Hansberg**, "Quantitative spatial economics," *Annual Review of Economics*, 2017, *9*, 21–58.

Rigaud, KK, B Jones, J Bergmann, V Clement, K Ober, J Schewe, S Adamo, B McCusker, S Heuser, and A Midgley, "Groundswell: Preparing for Internal Climate Migration (Washington, DC: World Bank)," 2018.

Rudik, Ivan, Gary Lyn, Weiliang Tan, and Ariel Ortiz-Bobea, "The Economic Effects of Climate Change in Dynamic Spatial Equilibrium," 2021.

Sotelo, Sebastian, "Domestic trade frictions and agriculture," *Journal of Political Economy*, 2020, *128* (7), 2690–2738.

Takeda, Kohei, "The Geography of Structural Transformation: Effects on Inequality and Mobility," 2022.

Veronese, N and H Tyrman, "MEDSTATII: Asymmetry in Foreign Trade Statistics in Mediterranean Partner Countries," Technical Report, Eurostat Methodologies Working Papers 2009.

Weiss, D, A Nelson, HS Gibson, W Temperley, S Peedell, A Lieber, M Hancher, E Poyart, S Belchior, N Fullman et al., "A global map of travel time to cities to assess inequalities in accessibility in 2015," *Nature*, 2018, *553* (7688), 333.

Appendix

Appendix A documents theoretical derivations that support the main results of Section 4. Appendix B describe alternative models used in the robustness. Appendix C provides more details about the data sources mentioned in Section 2 and other data sources not mentioned therein. Appendix D contains additional figures and tables.

A Theory Appendix

A.1 Derivation of shipping prices

The representative firm in location i uses labor as the unique input of a linear production technology. Locations trade with one another; following the iceberg-like formulation of trade costs, the quantity of a good from sector k produced by the representative firm from i shipped to location j is

$$q_{ij}^k = \frac{b_i^k A_i^k L_i^k}{\tau_{ij}}.$$

Thus, the representative firm solves

$$\max_{L_i^k} p_{ij}^k \frac{b_i^k A_i^k L_i^k}{\tau_{ij}} - w_i L_i^k \quad \forall k.$$

As a constant returns to scale problem, the solution is straight-forward: at an interior optimum, shipping prices will equal marginal shipping costs, i.e.

$$p_{ij}^k = \left(\frac{w_i}{b_i^k A_i^k}\right)\tau_{ij} \quad \forall i, j, k. \tag{A.1}$$

A.2 Derivation of bilateral trade shares

When maximizing welfare with respect to consumption of varieties, worker v solves

$$\max_{\{q_{ij}^k\}_{j,k}} \quad C_j \quad \text{s. to} \sum_{j\in\mathcal{S}}\sum_{k\in\mathcal{K}} p_{ji}^k q_{ji}^k \leq w_i \quad \forall i,$$

where C_j is (implicitly) defined in eq. (10) and the sectoral CES composites C_j^k in eq. (4). Then, taking the taking first order conditions of $\{q_{ij}^k\}_j$ to maximize utility

from sectoral k consumption, C_j^k, yields (μ stands for the Lagrange multiplier):

$$\frac{\eta_k}{\eta_k - 1} w_j^{1/\eta_k - 1} \frac{\eta_k - 1}{\eta} \left(q_{ij}^k\right)^{-1/\eta_k} - \mu p_{ij}^k \leq 0 \quad \forall i, j, \quad = 0 \text{ for interior solution. Assume so:}$$

$$\left(q_{ij}^k\right)^{\frac{-1}{\eta_k}} = \mu p_{ij}^k \times w_i^{1-\eta_k} \quad \forall i, j, \tag{A.2}$$

Then, the ratio of the consumption of two i and s varieties consumed at j becomes:

$$\frac{q_{ij}^k}{q_{sj}^s} = \left(\frac{p_{ij}^k}{p_{sj}^k}\right)^{-\eta_k} \quad \rightarrow \quad q_{ij}^k = \left(\frac{p_{ij}^k}{p_{sj}^k}\right)^{-\eta_k} \times q_{sj}^k \quad \forall i, j, s. \tag{A.3}$$

Then, by defining λ_{ij}^k as the share of j's expenditure on j's variety of sector k goods (and making use of eq. (A.3)), one obtains:

$$\lambda_{ij}^k = \frac{p_{ij}^k q_{ij}^k}{\sum_{s \in S} p_{sj}^k q_{sj}^k} = \frac{p_{ij}^k (p_{ij}^k / p_{sj}^k)^{-\eta_k} q_{sj}^k}{\sum_{s \in S} p_{sj}^k (p_{sj}^k / p_{ij}^k)^{-\eta_k} q_{sj}^k} = \left(\frac{p_{ij}^k}{P_j^k}\right)^{1-\eta_k} \quad \forall i, j,$$

where the last equation takes advatage of the definition of the price index from eq. (6). By proceeding analogously for the choice of crop composites (C_j^k) (middle CES nest) and the choice bewtween non-/agricultural composites (upper nest), one finds equivalent results to eqs. (8) and (12). Note that, for the latter, the derivation of the additional income effect follows Comin et al. (2021).

A.3 Derivation of migration shares

Take the definition of the welfare attained by a worker v living in i and moving to j as $W_{ij}(v) = (w_j / P_j) \bar{m}_{ij}^{-1} \varepsilon_j(v)$, $\varepsilon_i \sim G_j(v) = e^{-v^{-\theta} u_j L_j^{-\alpha}}$. Following Eaton and Kortum (2002), one can obtain the distribution of the welfare from one specific location i as

$$A_{ij}(w) \equiv \mathbb{P}(W_{ij} \leq w) = G_j(w P_j \bar{m}_{ij} / w_j) = e^{-(w P j \bar{m}_{ij} / w_j)^{-\theta} u_j L_j^{-\alpha}}.$$

Thus, the joint distribution of welfare of all destinations s from i can be derived as

$$A_i(w) = \prod_{s \in S} e^{-(w P_s \bar{m}_{is} / w_s)^{-\theta} u_s L_s^{-\alpha}} = e^{-\Phi_i \times w^{-\theta}}, \quad \text{where } \Phi_i = \sum_{s \in S} (P_s \bar{m}_{is} / w_s)^{-\theta} u_s L_s^{-\alpha}.$$

Now, recalling the share of workers moving from i to j is equivalent to the probability that the welfare attained by moving to j, w, is the highest among all other possible s

destinations, one writes

$$\Pi_{ij}(w) = \mathbb{P}\left(W_{ij}(v) \equiv w \geq \max\{W_{is}(v)\}_{s\neq j}\right) = \prod_{s\neq j}\mathbb{P}(W_{is} \leq w) = e^{-\Phi^{-j}\times w^{-\theta}}.$$

With that, it is possible to obtain the unconditional probability Π_{ij} by integrating over all possible values of $w \in \mathbb{R}_+$, i.e.

$$\begin{aligned}
\Pi_{ij} &= \int_0^\infty \Pi_{ij}(w)\; d\mathbb{P}(W_{ij} \leq w)\; dw \\
&= \int_0^\infty e^{-\Phi^{-j}\times w^{-\theta}} \times e^{(wP_j\bar{m}_{ij}/w_j)^{-\theta}u_jL_j^{-\alpha}} \times (-\theta)w^{-\theta-1}(P_j\bar{m}_{ij}/w_j)^{-\theta}u_jL_j^{-\alpha}\; dw \\
&= u_jL_j^{-\alpha}\left(\frac{P_j\bar{m}_{ij}}{w_j}\right)^{-\theta} \times \int_0^\infty e^{-\Phi_i\times w^{-\theta}}(-\theta)w^{-\theta-1}dw; \quad \text{multiply/divide by } \Phi_i \\
&= u_jL_j^{-\alpha}\left(\frac{P_j\bar{m}_{ij}}{w_j}\right)^{-\theta}\frac{1}{\Phi_i} \times \underbrace{\int_0^\infty \overbrace{e^{-\Phi_i\times w^{-\theta}}\Phi_i(-\theta)w^{-\theta-1}}^{dA(w)}dw}_{=1} \\
&= \frac{(w_j/P_j)^\theta\bar{m}_{ij}^{-\theta}u_jL_j^{-\alpha}}{\sum_{s\in S}(w_s/P_s)^\theta\bar{m}_{is}^{-\theta}u_sL_s^{-\alpha}},
\end{aligned}$$

which is the equivalent of eq. (17).

A.4 Numerical algorithm for solving the model

I find $\{w_j, L_j\}_{j\in S}$ that solves for the spatial equilibrium characterized by the system of equations (20) to (25) with an algorithm that nests three loops in one another.

Inner loop. I start with a guess for $\{w_j, L_j\}_j$ and solve for sectoral price indexes in eqs. (22) and (24). Then, with a guess for $\{P_j\}_j$, I iterate over eqs. (21) and (25) to find a simultaneous solution for $\{P_j, \mu_j^k\}_{j,k}$. In particular, with the guess for $\{P_j\}_j$, I solve for $\{\mu_j^k\}_k$ in eq. (25), replace it on eq. (21) to update solve for $\{P_j\}_j$, and iterate until both solutions converge.

Middle loop. I use the solution for $\{P_j, \mu_j^k\}_{j,k}$ and the guesses for $\{w_j, L_j\}_j$ in eq. (20) to obtain an update for $\{w_j\}_j$, iterating it until the solution converges.

Outer loop. I use the solution of $\{w_j, P_j\}_j$ and the guess for $\{L_j\}_j$ in eq. (23) to obtain an update for $\{L_j\}_j$, iterating it until the solution converges.

I then replace the solutions for $\{w_j, L_j\}_j$ back in the inner loop and repeat the procedure above until all solutions converge to a fixed point.

Existence and Uniqueness. My model is not isomorphic to the general set up of

Allen and Arkolakis (2014) and, as a consequence, the existence and uniqueness of the equilibrium cannot be guaranteed under their conditions for such. The reason for that is the additional non-linearity introduced by the middle- and upper-level CES structures. I address that by solving my model for several parametric choices, starting from many different initial guesses. The equilibrium found is invariant across all cases.

Winsorzing data and fundamentals. I winsorize both data and fundamentals when (i) bringing the model to the data (Appendix A.5) and (ii) solving the model with the calibrated geography. This procedure is standard as it removes the role of extreme values on the counterfactual results. Importantly, I check that such a procedure does not affect sensibly the equivalence between the calibrated model and the data that it fits. Appendix D.1 provides further details.

A.5 Model Inversion

The inversion of the spatial equilibrium consists of two steps that respectively back out fundamentals related to technology and location choice. Each of these steps consist of a two-stage procedure.

A.5.1 Technology

Its inner loop solves for $\{A_i^K\}_i$, $\{b_i^k\}_k$, and $\{\Omega_a, \Omega_K\}$ conditional on a guess for tariffs $\{\tau_{ij}^F\}$, the parameters taken from the literature, $\{A_i^k\}_{k\neq K}$ measured from GAEZ, and the observed following endogenous variables: real wages $\{w_i\}_i$, population $\{L_i\}_i$, sectoral production $\{X_i^k\}_{i,k}$, and aggregate sectoral expenditure ratios X^K/X^a.[47,48] Then, the outer loop matches model-generated bilateral country trade to observed data to pin down the levels of tariffs $\{\tau_{ij}^F\}$.

Inner loop. I use the market clearing condition of the model to build the equations

[47] All monetary values, built from the data in US$ PPP units (see Section 2), are further normalized to the wages of the first location w_1. This is done as I am not able to pin down levels in my quantification, but instead the spatial distribution of fundamentals up to a normalization.

[48] I reduce the role of outliers and extreme values in the data used in the inversion by winsorizing it. In particular, the observed real GDP per capita, $\{w_j\}_j$, is truncated at the 97,5th percentile. Moreover, the effective crop production, $\{X_j^k\}_{j,k\neq K}$, is truncated at the bottom and top quartiles within countries.

for nominal GDP, sectoral wage bills, and aggregate sectoral expenditure shares:[49]

$$w_j L_j = \sum_{i \in S} \sum_{k \neq K} \lambda_{ji}^k \Xi_i^k \mu_i^a w_i L_i + \sum_{i \in S} \lambda_{ji}^K \mu_i^K w_i L_i \tag{A.4}$$

$$X_j^k = \sum_{i \in S} \lambda_{ji}^k \Xi_i^k \mu_i^a w_i L_i \quad \forall k \neq K \tag{A.5}$$

$$X_j^K = \sum_{i \in S} \lambda_{ji}^K \mu_j^K w_i L_i \tag{A.6}$$

$$X_K / X_a = \frac{\sum\limits_{j \in S} \sum\limits_{i \in S} \lambda_{ji}^K \mu_i^K w_i L_i}{\sum\limits_{k \neq K} \sum\limits_{j \in S} \sum\limits_{i \in S} \lambda_{ji}^k \Xi_i^k \mu_i^a w_i L_i}. \tag{A.7}$$

Then, one can invert each of the equations above to obtain the expressions for the unobserved fundamentals of interest. For instance, for $\{A_j^K\}_j$, one inverts eq. (A.4) to obtain:

$$w_j L_j = \sum_{i \in S} \sum_{k \neq K} \lambda_{ji}^k \Xi_i^k \mu_i^a w_i L_i + \sum_{i \in S} \left(\frac{w_i \tau_{ji}}{b_j^K A_j^K P_i^K} \right)^{1-\eta_K} \mu_i^K w_i L_i \rightarrow$$

$$A_j^K = \left[\frac{w_j L_j - \sum\limits_{i \in S} \sum\limits_{k \neq K} \lambda_{ji}^k \Xi_i^k \mu_i^a w_i L_i}{\sum\limits_{i \in S} \left(w_i \tau_{ji} / b_j^K P_i^K \right)^{1-\eta_K} \mu_i^K w_i L_i} \right]^{\frac{1}{\eta_K - 1}}. \tag{A.8}$$

Analogously inverting eqs. (A.5) to (A.7) yields:

$$b_j^k = \left[\frac{X_j^k}{\sum\limits_{i \in S} \left(w_j \tau_{ji} / A_j^k P_i^k \right)^{1-\eta_k} \Xi_i^k \mu_j^a w_i L_i} \right]^{1/(\eta_k - 1)} \quad \forall k \neq K \tag{A.9}$$

$$b_j^K = \left[\frac{X_j^K}{\sum\limits_{i \in S} \left(w_j \tau_{ji} / A_j^K P_i^K \right)^{1-\eta_K} \mu_j^K w_i L_i} \right]^{1/(\eta_K - 1)} \tag{A.10}$$

$$\Omega_K / \Omega_a = \frac{X^K}{X^a} \times \frac{\sum\limits_{k \neq K} \sum\limits_{j \in S} \sum\limits_{i \in S} \lambda_{ji}^k \Xi_i^k \left(P_i^a / P_i \right)^{1-\sigma} \left(w_i / P_i \right)^{\varepsilon_a - (1-\sigma)} w_i L_i}{\sum\limits_{j \in S} \sum\limits_{i \in S} \lambda_{ji}^K \left(P_i^K / P_i \right)^{1-\sigma} \left(w_i / P_i \right)^{\varepsilon_K - (1-\sigma)} w_i L_i}. \tag{A.11}$$

The inversion algorithm finds $\{A_j^K, \{b_j^k\}_{j,k}, \Omega_K / \Omega_a\}$ such that eqs. (A.8) to (A.11) hold simultaneously. However, because $\{b_j^K\}_j$ and $\{A_j^K\}_j$ cannot be separated out in

[49] By targetting the relative sectoral expenditures, I am implicitly normalizing one of the preference shifters to one and indentifying their ratio.

levels, I do normalize the latter to one and identify the product of them in eq. (A.10). That also gives me tractability, as then eq. (A.8) is not needed anymore for inverting the spatial equilibrium.[50]

I solve for the fundamentals as follows: with a guess for $\{b_j^k\}_{j,k}$, I solve for Ω_K/Ω_a in eq. (A.11). I then plug the solution in eqs. (A.9) and (A.10) (embedded in $\{\mu_j^k\}_{j,k}$) to solve for $\{b_j^k\}_{j,k}$. I iterate it until all solutions converge.

Outer loop. The inner loop uses a guess of the tariff parameter τ_{ij}^F, which the outer loop solves for. In particular, it repeats the inner loop for a range of $\tau_{ij}^F \in \{1, 1.05, ..., 3\}$ and finds $\tau_{ij}^F = 2.175$ to be the value such that the model-generated international trade flows, $X^F = \sum_{j\in S}\sum_{i\notin c(j)} X_{ji}$, matches the observed data from the ITPD-E (Borchert et al., 2021).[51]. Figure A.1 shows the results of the grid search.

A.5.2 Location choice

Its inner loop solves for $\{u_i\}_i$ and $\{m_c\}_c$ conditional on all previsouly quantified parameters and fundamentals, a guess for ϕ, and the observed following endogenous variables: population $\{L_i\}_i$ and country-level total inflow of foreign migrants, $\{L_c\}_c$ (obtained from Abel and Cohen (2019)'s database). Then, the outer loop matches model-generated total internal migration to observed data to pin down ϕ.

Inner loop. I use eq. (18) to calculate L_c. Then, I analogously invert that to obtain an expression for country barriers as a function of L_c and other endogenous variables and fundamentals as follows:

$$L_c = \sum_{j\in c}\sum_{i\notin c} \frac{\left(w_j/P_j\right)^\theta m_{ij}^{-\theta} m_{c(j)}^{-\theta} u_j}{\sum\limits_{s\in c(j)} \left(w_s/P_s\right)^\theta m_{is}^{-\theta} u_s + \sum\limits_{s\notin c(j)} \left(w_s/P_s\right)^\theta m_{is}^{-\theta} m_{c(s)}^{-\theta} u_s} L_{i0} \rightarrow$$

$$m_c = \left[L_c^{-1} \times \sum_{j\in c}\sum_{i\notin c} \frac{\left(w_j/P_j\right)^\theta m_{ij}^{-\theta} u_j}{\sum\limits_{s\in c(j)} \left(w_s/P_s\right)^\theta m_{is}^{-\theta} u_s + \sum\limits_{s\notin c(j)} \left(w_s/P_s\right)^\theta m_{is}^{-\theta} m_{c(s)}^{-\theta} u_s} L_{i0} \right]^{1/\theta} \tag{A.12}$$

Note that the denominator in the equations above is equivalent to eq. (18)'s – it separates the inter/intranational bilateral choices to illustrate the identification of parameters later on. Analogously, I invert eq. (23) to pin down amenities $\{u_j\}_j$ as a function

[50] In particular, that equation holds by construction if eqs. (A.9) and (A.10) hold simultaneously.

[51] In practice, as I do not identify levels in the inversion, I match the share of exports over total SSA GDP

of population distribution and other endogenous variables and fundamentals:

$$u_j = L_j \times \left[\sum_{i \in c(j)} \frac{\left(w_j / P_j\right)^{\theta} m_{ij}^{-\theta}}{\sum_{s \in c(j)} \left(w_s / P_s\right)^{\theta} m_{is}^{-\theta} u_s + \sum_{s \notin c(j)} \left(w_s / P_s\right)^{\theta} m_{is}^{-\theta} m_{c(s)}^{-\theta} u_s} L_{i0} + \sum_{i \notin c(j)} \frac{\left(w_j / P_j\right)^{\theta} m_{ij}^{-\theta} m_{c(j)}^{-\theta}}{\sum_{s \in c(j)} \left(w_s / P_s\right)^{\theta} m_{is}^{-\theta} u_s + \sum_{s \notin c(j)} \left(w_s / P_s\right)^{\theta} m_{is}^{-\theta} m_{c(s)}^{-\theta} u_s} L_{i0} \right]^{-1} \tag{A.13}$$

I solve eqs. (A.12) and (A.13) as follows: with a guess for $\{u_j\}_j$, I solve for $\{m_c\}_c$ in eq. (A.12), plug it in eq. (A.13) to solve for $\{u_j\}_j$, and iterate it until all solutions converge. Importantly, I am able to separate out $\{u_j\}_j$ from $\{m_c\}_c$ because location pairs can refer to either intra or international migration. That is, conditional on a guess of $\{u_j\}_j$, there are distinct origins s for which a destination j stand for one type of migration of the other (the denominator of eq. (A.12)), and thus where amenities multyplies or not the country migration barriers $\{m_c\}_c$. Considering all possible origins s and destinations j in S, there is at least one pair for which they do and do not multiply one another, which then allows me to separately identify them.

Outer loop. The inner loop uses a guess for ϕ, which the outer loop solves for. In particular, it repeats the inner loop for a range of $\phi \in \{0, 0.05, ..., 1.5\}$ and finds $\phi = 0.5$ to be the value such that the model-generated internal migration flows, $L^D = \sum_{c \in C} \sum_{j \in c} \sum_{i \in c} L_{ij}$, matches the observed internal migation flows between 1990 and 2000. Importantly, Abel and Cohen (2019) do not provide data on internal migration. Thus, I rely on policy reports and other evidence to find that the approximated total internal migration flows in SSA between 1990 and 2000.[52]. I find it to be 50 million of individuals and thus target this value in the quantification of ϕ. Figure A.1 shows the results of the grid search.

A.6 Discussion of the parameters taken from the literature

Lower CES tier. The values taken for $\{\eta_k\}_k$ come from Pellegrina and Sotelo (2021); Caliendo and Parro (2015). While initially used in Caliendo and Parro (2015) at the country level, Pellegrina and Sotelo (2021) use the same values to study intranational trade and migration in rural Brazil by mid 20th century (which is a good approximation of rural SSA as of 2000). Assuming different values for $\{\eta_k\}_k$ (say, substitution of varieties within countries being more intense than across countries) would mainly

[52] In particular, Myers (1993, 1997, 2002) suggest that climate displaced individuals by the end of the 20th century in SSA were in the order of 52 million. Gemenne et al. (2022) instead suggest internal migration flows in the order of 25 million. Finally, Brown et al. (2007), basing upon sources such as Myers (2002) or UNHCR (UN's Refugee Agency) suggests flows in the order of 60 million.

Figure A.1: Results of the outer loops that solve for τ_{ij}^F and ϕ

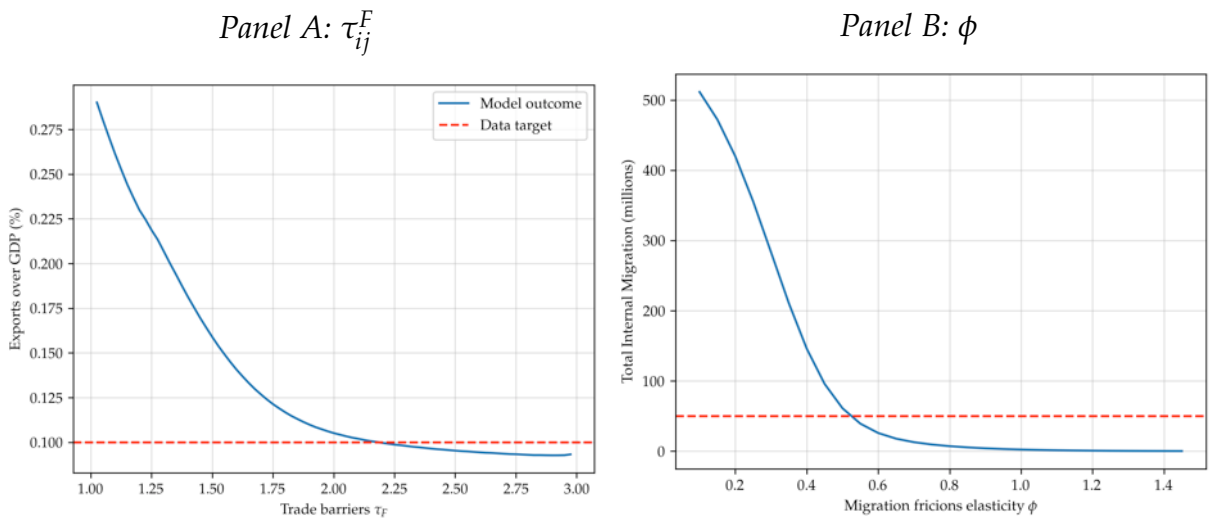

Notes: Panel A: Grid search over τ_{ij}^F (x-axis) and the resulting model-generated international trade flows (y-axis). The dashed red line stands for the target of the observed trade flows in the data. Panel B: analogous grid search over ϕ and the resulting model-generated internal migration flows.

affect the model-generated trade flows, and consequently the parameters associated to trade frictions.

Middle CES tier. The value $\gamma_a = 2.5$ comes from Sotelo (2020), who studies rural Peru by early 2000s and focus on intranational trade in that country. Thus, it stands for a context similar to rural SSA as of 2000.

Upper CES tier. The values for $\{\varepsilon_k\}$ and σ come from the global estimation of Nath (2022). The parameters therefore reflect preferences between agricultural and non-agricultural goods from a global representative consumer. Thus, the values can underestimate the subsistency aspect of agricultural goods in SSA, where the negative slope of the Engel curve could be steeper vis-à-vis the rest of the world. If so, then, my results would underestimate the welfare losses associated to that mechanism.

A.7 Details on the Backcasting Exercise for 1975

The backcasting exercise consists of solving for the spatial equilibrium of the SSA in 1975. In particular, it uses the calibrated model for 2000 and replaces two fundamentals that reflect the reality of the economy in 1975:

Population. I calculate and estimate of the initial population in 1975 by projecting the distribution of the observed population in 2000 into the levels of the SSA population in 1975. The reversibility of the spatial equilibrium follows Desmet et al. (2018), who characterize the possibility of backcasting exercises such as mine (i.e. validating spatial models calibrated in a cross section).

Crop yields. I replace the fundamental productivities $\{A_j^k\}_{k \neq K}$ used in the calibration with the values of 1975. Importantly, during the period there was already climate-driven changes in these productivities so that the model can generate climate migration. Figure A.2 illustrates that.

Figure A.2: Percentual changes in average crop potential yields within locations in the past and estimates for the future

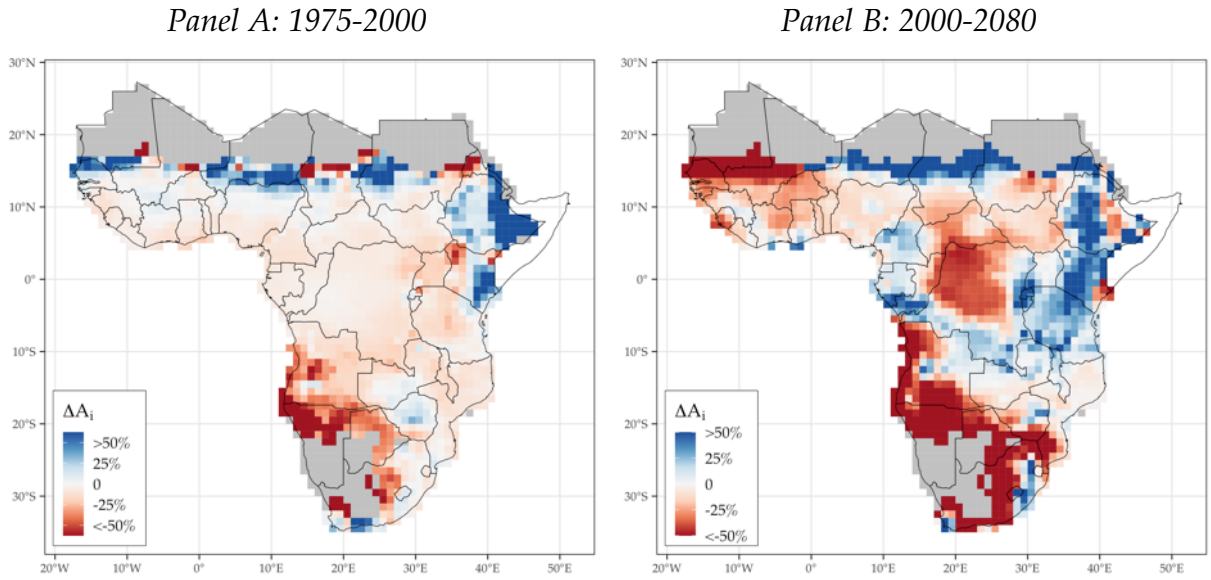

Notes: Panel A: Within grid cell changes (%) in crop suitabilities between 1975 and 2000. Panel B: Analogous changes between 2000 and 2080 (under climate change). Grey areas stand for locations with no zero potential yields in both periods.

Finally, the validating exercises consists of comparing the model outcomes with observed population data for 1975. Because the data source of the latter (GHSP, Florczyk et al., 2019) differs from the source of population data used in the calibration (G-Econ, Nordhaus et al., 2006), I check the consistency of these two datasets for the period of 2000 (for which data in both sources is available) in terms of grid cell- and country-level population correlation.

A.8 Details on the calibration with EU data

I take the model to EU data so to retrieve the levels of the tariffs and country barriers paramters τ_{ij}^F and $\{m_c\}_c$. To do that, I build a likewise rich spatial dataset for the EU. I use the same sources described in Section 2, as all of them have a global coverage.

Subsequently, I link that data to my model with the procedure described in Section 5. Importantly, when doing so, I use the same preference parameters and elasticities to bilateral distance, δ and ϕ. Thus, my quantification for the EU embeds the differences between cross country trade (or migration) in EU and SSA in the policy parameters τ_{ij}^F (or $\{m_c\}_c$).

Figure A.3: Correlations between populations from G–Econ and GHSP datasets for the year of 2000

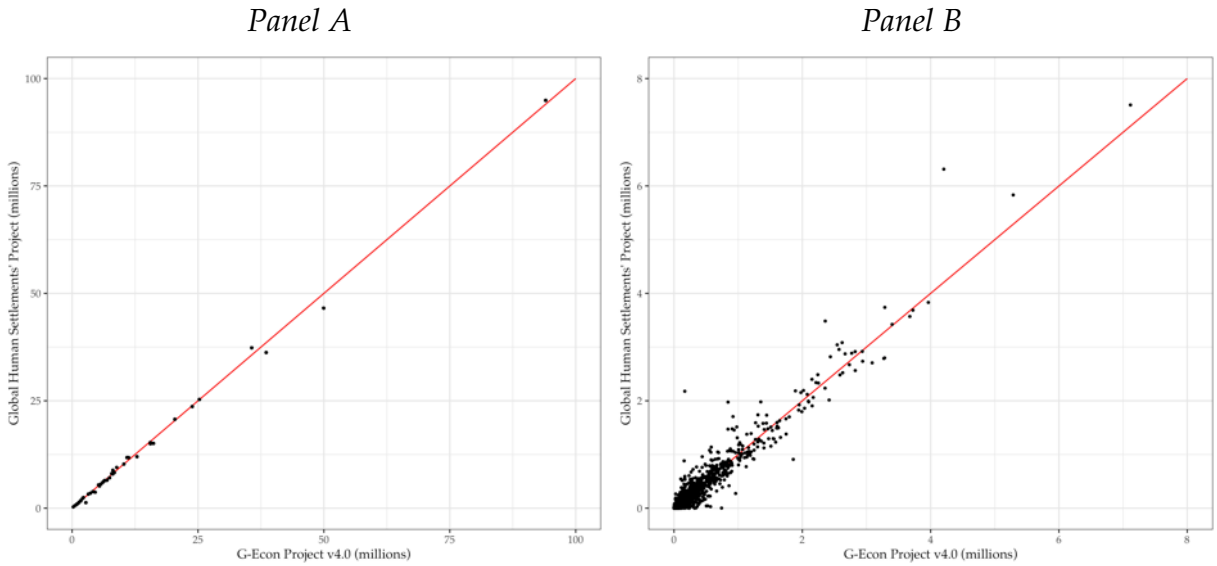

Notes: Panel A: Population counts in SSA from G–Econ (x axis) and GHSP (y axis) aggregate at country level. Panel B: Population counts in SSA from G–Econ (x axis) and GHSP (y axis) aggregate at 1 degree grid cells.

Finally, when replacing the EU policy parameters into the SSA counterfactual, I must match the country level EU parameters $\{m_c\}_c$ to SSA countries. I do that by quantiles. That is, I assign the country barrier value for the bottom decile of the EU sample to the countries in the bottom decile of the SSA county barrier distribution, as so forth for the other deciles. Importantly, to make the levels of $\{m_c\}_c$ comparable across EU and SSA, I normalize the former as a ratio with the minimum. Thus, I in practice simply scale SSA's country barriers in relatives (e.g. the ratio between the least and most strict country) so to reflect the relative ratios of the EU barriers.

B Alternative models

B.1 Agriculture as a unique crop

The model with a unique crop is identical to the model of Section 4. However, by assuming a unique crop ($K = 2$), there is no subsitution within agriculture, so that the middle CES tier vanishes (i.e. $\Xi_j^1 = 1$ and $P_j^a = P_j^1$ for all j).

I take this model to the data following the procedure described in Section 5. The only difference from the baseline model is that the unique crop is an aggregate of the 6 crops. In particular, the agricultural fundamental productivity $\{A_j^k\}_{k \neq K}$ is a cross-crop average of the within grid cell productivities (and likewise for the 2080 estimates). Moreover, the crop expenditures used in the baseline quantification are

summed up for the single-crop case.

B.2 Homothetic preferences

I model homothetic preferences in a simple model where crops and non-agricultural goods are imperfect substitutes. That is, I assume a two-level CES structure where the lower nest is identical to the baseline. The upper nest, instead, is a CES aggregator of both crops and non-agricultural CES composites:

$$C_j = \sum_{k \in K} \left(\left(C_j^k \right)^{(\sigma-1)/\sigma} \right)^{\sigma/(\sigma-1)}$$

The spatial equilibrium with this simpler model is characterized by $\{w_j, L_j\}_j$ such that the following system holds:

$$w_i L_i = \sum_{j \in S} \sum_{k \in \mathcal{K}} (P_j^k / P_j)^{1-\eta} \left(\frac{w_i \tau_{ji}}{b_i^k A_i^k P_j^k} \right)^{1-\sigma} w_j L_j \tag{B.1}$$

$$L_j = \sum_{i \in S} \frac{(w_j / P_j)^{\theta} \bar{m}_{ij}^{-\theta} u_j L_j^{-\alpha}}{\sum_{s \in S} (w_s / P_s)^{\theta} \bar{m}_{is}^{-\theta} u_s L_s^{-\alpha}} \times L_i^0 \tag{B.2}$$

$$P_i^k = \left(\sum_{j \in S} (w_j \tau_{ji} / b_i^k A_j^k)^{1-\sigma} \right)^{\frac{1}{1-\sigma}} \tag{B.3}$$

$$P_i = \left(\sum_{k \in \mathcal{K}} \left(P_i^k \right)^{1-\eta} \right)^{\frac{1}{1-\eta}} \tag{B.4}$$

When taking this model to the data, I use $\sigma = 2.5$ following Sotelo (2020) and follow almost the same procedure as in Section 5. The only difference in this case is that I disregard the parameters related to the upper tiers of the baseline model (i.e. $\{\Omega_j^k\}_k$). In practice, that means matching only sectoral output in the inversion for the fundamentals related to the technology (eqs. (A.8) to (A.10) in appendix A.5.1).

B.3 Endogenous fertility

I endogenize fertility, with respect to climate change, with a simple damage function that assumes that the projected grid-cell-level initial population for 2080 is affected by the average change in local crop yields. Formally:

$$\hat{L}_j^0 = (\iota \times \Delta A_j) \times L_j^0,$$

where ΔA_j is the average crop yield change in j (as in Section 3) and ι a shitfer that maps the latter into fertility changes.

When doing so, the initial population of SSA $\mathcal{L}$ reduces dramatically if compared to the baseline case. In particular, it decreases more in the locations and countries

that are most affected by climate change. Thus, in distributional terms, the initial population of SSA starts better distributed, which leads to lower climate migration flows. Moreover, because of the lower level of aggregate population, there are less congestion forces in the economy (driven by α), which allows more people, in relative terms, to move into the best locations in the economy (compared to the baseline simulations).

The fertility robustness results of Table 5 use $\hat{L}_j^0$ and $\iota = .5$ in the climate change simulations. As of completeness, Table B.1 below document how these results are sensitive to the choice of ι.

Table B.1: Robustness of the endogenous fertility exercise with respect to ι

	(1) Climate migration (million individuals)	(2) Δ GDP per capita (%)	(3) Δ Non–agricultural employment (%)
Endogenous fertility $\iota = 0.1$	2.55	2.71	1.76
Endogenous fertility $\iota = 0.25$	2.54	2.71	1.76
Endogenous fertility $\iota = 0.5$	2.52	2.72	1.77

C Data Appendix

Table C.1 below documents all data sources used and their temporal coverage. Next, I provide further detail on the data choices and aggregation.

Table C.1: Main data sources

Type of data	Coverage	Source
GDP and Population	2000	G-Econ Project v4.0 (Nordhaus et al., 2006)
Population	1975, 2000	Global Human Settlements Project (Florczyk et al., 2019)
Population projections	2021 – 2100	United Nations and Social Affairs (2019)
Agric. Productivities	1960–2000	GAEZ v3.0 (IIASA and FAO, 2012)
Climate Δ projections	2020, 2050, 2080	GAEZ v3.0 (IIASA and FAO, 2012)
Transportation data	2000	gROADS project (CIESIN, 2013)
Friction transportation surface	2000	Accessibility to Cities' project (Weiss et al., 2018)
Bilateral crop trade data	1995–2005	ITPD-E (Borchert et al., 2021)
Bilateral country migration data	1990–2000	Abel and Cohen (2019)

C.1 GAEZ agro-climatic yields.

The GAEZ's database provides estimates of agricultural potential yields for several crops, in different time periods, and for different degrees of technology usage in agriculture. As my interest in subsistence agriculture setup of SSA, I aim at building a

Figure C.1: Yield gains from adoption of high inputs in agriculture vis–à–vis low inputs for selected crops.

Panel A: Gains for adoption of high inputs for rice

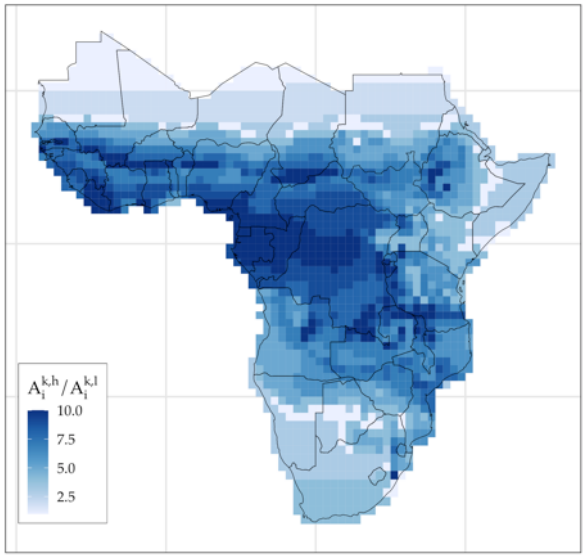

Panel B: Gains for adoption of high inputs for sorghum

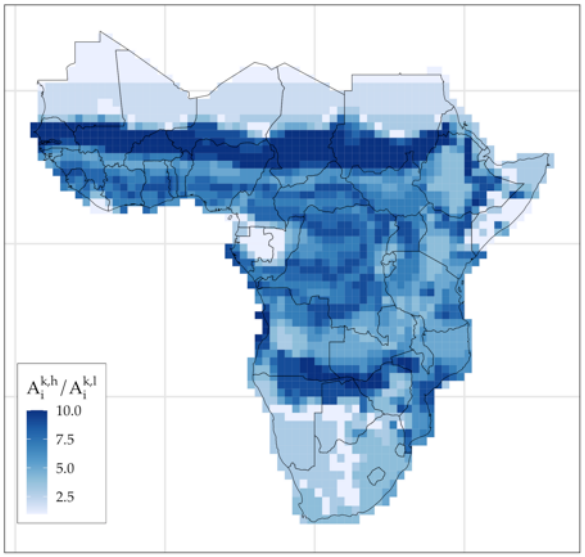

Notes: Panels A and B show the ratio of high/low input usage yields for growing two selected crops according to GAEZ long–run estimates. The values are shown in deciles; 1 (10) stands for the bottom (top) decile of each sample.

time varying dataset of potential yields over the entire subcontinent, for several crops, at low usage of modern inputs: with rainfed water access, labor intensive techniques, and no application of of nutrients, no use of chemicals for pest and disease control and minimum conservation measures.

A challenge, however, is that the time varying potential yields from GAEZ are available only for high usage of modern inputs (based on improved high yielding varieties, fully mechanized with low labor intensity techniques, and usage of optimum applications of nutrients and chemical pest, disease and weed control). The estimates for different input levels are only available for the long–run estimates (averages between 1960–1990).

Therefore, to obtain a time varying dataset of the agro–climatic yields at low input usage, I first use the long–run values to calculate the GAEZ–implied ratio between high inputs $(A_i^{k,h})$ / low inputs $(A_i^{k,l})$ yields for each crop. This procedures reveals how the gains from adopting higher input levels differ across locations and crops – Figure C.1 illustrates the results for two selected crops in deciles. I use the calculated ratios to scale down the time varying estimates for high inputs that I collect.

Armed with the location–crop technology scales, I collect the time varying estimates of agro–climatic yields for high input usage. For the estimates in the past, retrieve those for 1971–1975 and 1996–2000. I average out the 5 years' blocks so to avoid year-specific outliers. The reason is to capture long term changes, which could

Figure C.2: Equivalence between long and longer–run estimates of radiative forcing (proportional to carbon emissions) between SRES and RCP scenarios.

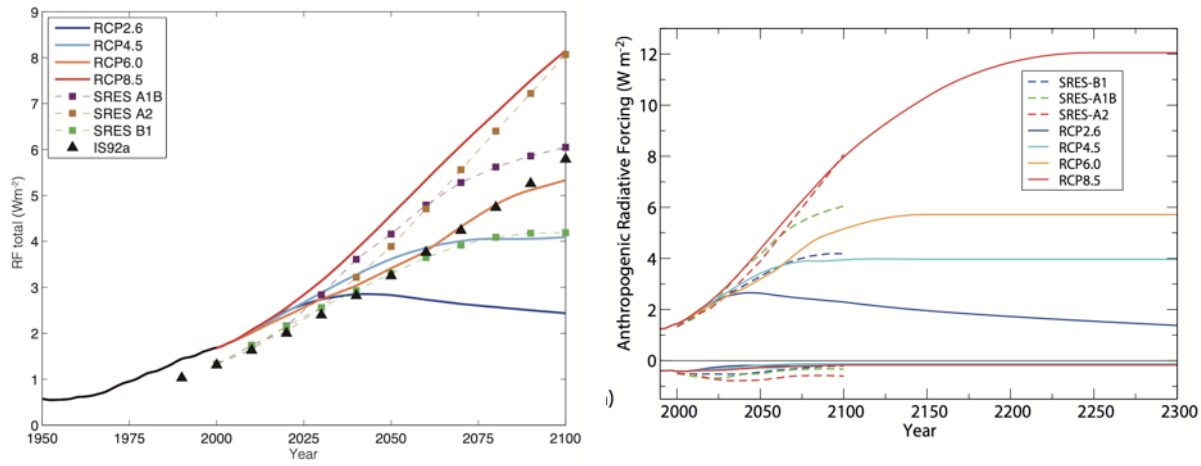

Source: IPCC (2012), chapter 1, Figure 1.15 (left) and Chapter 12, Figure 12.3 (right).

be contaminated if a certain year faces unusual climate conditions.

The yield estimates for future periods require another parametrical selection: the underlying scenario for which the data is produced and with which climatic (general circulation) model (GCM) the data is produced. As carefully discussed by Costinot et al. (2016), the GAEZ v3.0 database provides such estimates produced with four main GCM, and for several future scenarios. The latter is of key importance: it contains the underlying assumption on how the global carbon emissions are going to evolve in the future so to produce the changes in the climate.

I choose the scenario A1 from the GAEZ database, which is the baseline scenario of Costinot et al. (2016) that matches closely the current standard of severe evolution of the global climate for the future: the RCP 8.5.[53] This scenario assumes a steady increase in carbon stocks in the atmosphere througout the 21st and 22nd centuries, becoming stable by mid–23rd century. A milder scenario that I use for my robustness checks is the B1, which is similar to the nowadays–standard RCP 4.5. It assumes that the global stock of carbon will peak by late 21st century, becoming stable thereafter.

C.2 ITPD-E data.

The trade data used in this paper is obtained from the ITPD-E database (Borchert et al., 2021). I collect all available bilateral trade flows, in current US$, for all country-crops combinations of my study.

[53]The GAEZ v3.0 forecasts are based on the Special Report on Emission Scenarios (SRES; see IPCC, 2000). The SRE Scenarios were later updated by IPCC as the RCP scenarios, which are now the standards in the climate community (IPCC, 2012). Figure C.2 illustrates the equivalence between the SRES and RCP scenarios.

Consistent with good practice with trade data, I collect import flows rather than exports. The reson for that is the usual discrepancy between total import and exports at the country–pair–product level. While import flows are registered between country of production and final country of shipment, export data usually register intermediate countries on the trade chain as final destination, biasing the trade flows (Veronese and Tyrman, 2009).

Finally, to transform the trade data to monetary unit of my study (US$ PPP from G–Econ), I proceed as follows. First, I calculate the share of trade flows, at the importer–exporter–crop–year levels, over the GDP of of the importing country in each year, in current values. Subsequently, I average out the shares over the 2000–2010 period, so to avoid outliers in the year of 2000. Finally, I multiply the shares at the importer–exporter–crop level by the importer GDP of G–Econ for the year of 2000.

C.3 Building the agricultural production data.

To build a dataset for agricultural production at the location–crop level for 2000, I combine the GAEZ data of production (in tonnes) with the FAOSTAT agricultural production data (country–crop level) and World Bank country GDP data (both in current US$). First, I use the GAEZ data at the cell–crop level to calculate the share that each cell is observed to produce, of each crop, over its country's total production. Second, I obtain with the FAOSTAT and WB data the share of each country crop production for the years of 2000 to 2010. I average out such shares and multiply them by the country GDP implied by the G–Econ data, so that the unit is consistent with the monetary unit of the model (US$ PPP). Finally, I multiply the country–crop PPP values by the location–crop shares. For very liitle locations, however, the outcome can exceed the their total GDP. In these cases, I simply trim the value by 99.99% of its GDP.

C.4 Additional data sources

Main populated places. I collect the coordinaes of the main populated places of SSA from the Populated Places data set from Natural Earth. It consists of a geo-referenced dataset with the coordinates of about 90% of all cities, towns and settlements in the World. I use it to set coordinates for each of the cells of SSA. If a certain cell contains more than one location, I pick the one with the highest population. If another does not have any location to obtain the coordinates, I set them to be the cell's centroid. Finally, if any of the centroids are not located in the mainland (i.e. ocean, lakes), I set it to be the closest coordinate to the centroid that is on the mainland. See fig. D.3 for the result.

D Additional material

D.1 Further details on winsorizing and the spatial aggregation method

D.1.1 Winsorizing of data and fundamentals

The calibration of the geography $\mathcal{G}(S)$ for 2000 fits perfectly the observed data for that period. Therefore, the quantified fundamentals incorporate all possible measurement error present in the data. I address it by, first, winsorizing the data used in the inversion as explained in Appendix A.5 (see footnote 48). However, that procedure does not eliminte fully the extreme outliers obtained in the fundamentals, especially with respect to the efficiency shifters $\{b_j^k\}_{j,k}$. Thus, when solving the model for any simulation using the calibrated model, I also winsorize $\{b_j^k\}_{j,k}$ at the 97.5% percentile.

Importantly, doing so does not affect sensibly the equivalence between the calibrated model and the observed data. For instance, there are nearly no differences between the results of the validation of Section 5.6 with the actual fundamentals and the winsorized ones. Figure D.1 illustrates that, and Table D.1 document the sensitivity of the climate change counterfactuals to that.

Figure D.1: Backcasting exercise with and without winsorizing of $\{b_j^k\}_{j,k}$

Panel A: Backcasting with winsorizing *Panel B: Backcasting without winsorizing*

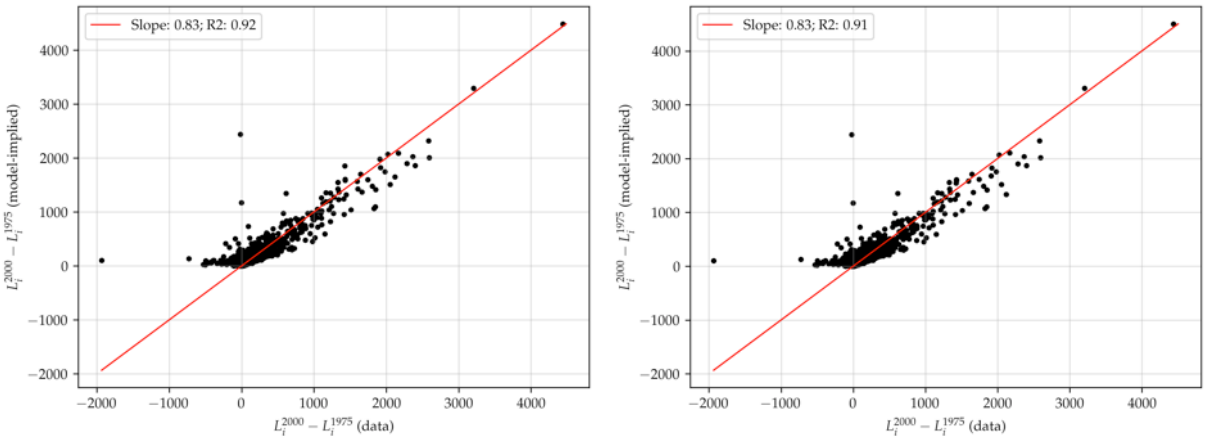

Notes: Observed (x-axis) and model-generated (y-axis) population changes between 2000 and 1975. Panel A shows the results if winsorizing the fundamentals, and Panel B if not.

D.1.2 Spatial aggregation of GAEZ data

As discussed in Section 6.1 (see footnote 34), Appendix A.4, and Appendix C.1, I choose and aggregate the GAEZ estimates of crop yields for 2080 so to capture the most pessimistic scenario available. The first choice in that direction is to choose the scenario available at GAEZ that reflects the closest the RCP 8.5 scenario (see

Appendix C.1). Several sources (data generated using a specific Global Circulation Model – GCM), for that scenario, are available. For consistency with the literature and comparability, I choose the one from Costinot et al. (2016) (Hadley CM3).

However, the Hadley CM3 forecasts differ sensibly from other sources. Again in line with the principle of capturing the most pessimistic possible future scenario, I aggregate the raw GAEZ data for 2080 centered at the bottom 5th percentile of the within-grid cell distribution. Thus, my results reflect an upper bound in terms of magnitudes of losses. [54] Figure D.2 shows the sensitivity of the average crop yield changes (equivalent to Figure 1 Panel A) with respect to this aggregation method. Moreover, Table D.1 document how the aggregate baseline results change if using other methods. Intuitively enough, choosing a less pessimistic rule reverts the aggregate welfare losses of climate change by providing more room for sectoral specialization (more agricultural production centered in the benefitted areas).

Figure D.2: Sensitivity of ΔA_i with respect to the spatial aggregation rule - 5th and 25th percentiles, and average changes

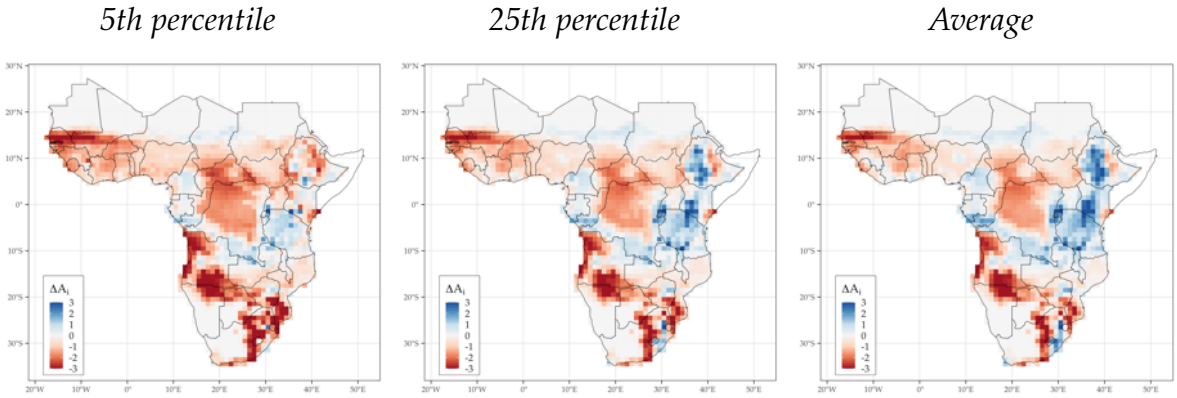

Table D.1: Sensitivity of the climate change counterfactuals to truncation of fundamentals and spatial aggregation

	(1) Climate migration (million individuals)	(2) Δ GDP per capita (%)	(3) Δ Non–agricultural employment (%)
Aggregation at 5th percentile (baseline)	4.02	-1.18	-0.85
Aggregation at 25th percentile	2.58	2.71	1.76
Aggregation at the mean + no truncation of $\{b_j^k\}_{j,k}$	3.44	5.33	5.82

[54] By targetting an upper bound of climate losses, I do not need to check the sensitivity of my results to all different GCM sources provided by GAEZ.

D.2 Further results

Table D.2: Share of grain crop production (in tonnes) over total production of the main staple and cash crops in SSA.

Crop	Share of production
Grain crops:	
Cassava	56.65%
Maize	11.75%
Millet	4.59%
Rice	2.18%
Sorghum	6.15%
Wheat	1.13%
Total:	82.45%
Cash crops:	
Coffee	1.13%
Cotton	1.14%
Groundnut	2.72%
Palm oil	4.93%
Soybean	0.33%
Sugarcane	7.31%
Total:	17,55%

Source: GAEZ production data for 2000 aggregated in over the 42 countries of my empirical setup. SSA includes all sub–Saharan African countries but Somalia.

Figure D.3: Coordinates for SSA grid cells (localities) for Western (left) and Eastern (right) Africa.

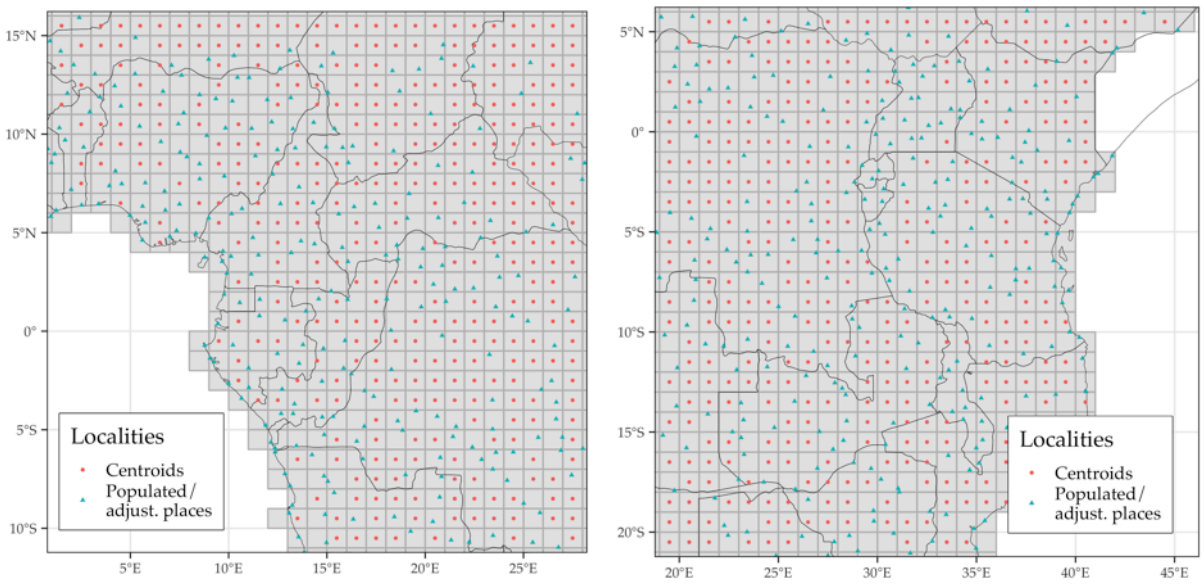

Table D.3: Climate migration results for country capitals

Country	Capital	ΔL_i (K)	Country	Capital	ΔL_i (K)
Angola	Luanda	41.89	Lesotho	Maseru	-14.27
Burundi	Bujumbura	-25.33	Mali	Bamako	141.06
Benin	Cotonou	-11.39	Mozambique	Maputo	66.75
Burkina Faso	Ouagadougou	45.17	Mauritania	Nouakchott	56.29
Botswana	Gaborone	0.79	Malawi	Lilongwe	-43.38
Central African Republic	Bangui	17.80	Namibia	Windhoek	9.43
Ivory Coast	Abidjan	96.35	Niger	Niamey	-55.70
Cameroon	Yaounde	16.67	Nigeria	Abuja	48.62
Congo (Kinshasa)	Kinshasa	830.26	Rwanda	Kigali	735.19
Congo (Brazzaville)	Pointe-Noire	22.34	Sudan	Khartoum	21.60
Djibouti	Djibouti	0.34	Senegal	Dakar	179.32
Eritrea	Asmara	10.03	Sierra Leone	Freetown	-101.60
Ethiopia	Addis Ababa	12.83	Swaziland	Mbabane	4.50
Gabon	Libreville	9.25	Chad	Ndjamena	-5.23
Ghana	Accra	-111.79	Togo	Lome	10.24
Guinea	Conakry	0.76	Tanzania	Dar es Salaam	63.87
The Gambia	Banjul	-47.31	Uganda	Kampala	-7.74
Guinea Bissau	Bissau	-2.42	South Africa	Johannesburg	-25.18
Equatorial Guinea	Malabo	0.55	Zambia	Lusaka	24.38
Kenya	Nairobi	341.50	Zimbabwe	Harare	-1.38
Liberia	Monrovia	31.47			